N62711491

NASA TN D-917

IN-53
38787

TECHNICAL NOTE

D-917

A FIXED-BASE-SIMULATOR STUDY OF THE ABILITY OF A PILOT TO ESTABLISH CLOSE ORBITS AROUND THE MOON

By M. J. Queijo and Donald R. Riley

Langley Research Center
Langley Field, Va.

NATIONAL AERONAUTICS AND SPACE ADMINISTRATION
WASHINGTON June 1961

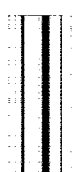

NATIONAL AERONAUTICS AND SPACE ADMINISTRATION

TECHNICAL NOTE D-917

A FIXED-BASE-SIMULATOR STUDY OF THE ABILITY OF A PILOT TO ESTABLISH CLOSE ORBITS AROUND THE MOON

By M. J. Queijo and Donald R. Riley

SUMMARY

A study was made on a six-degree-of-freedom fixed-base simulator of the ability of human pilots to modify ballistic trajectories of a space vehicle approaching the moon to establish a circular orbit about 50 miles above the lunar surface. The unmodified ballistic trajectories had miss distances from the lunar surface of from 40 to 80 miles, and a velocity range of from 8,200 to 8,700 feet per second at closest approach. The pilot was given control of the thrust (along the vehicle longitudinal axis) and torques about all three body axes. The information display given to the pilot was a hodograph of the vehicle rate of descent and circumferential velocity, an altimeter, and vehicle attitude and rate meters.

The general procedure used in the investigation was to permit the pilots to become familiar with the instrumentation, controls, and indicated vehicle dynamics by flying a simple "nominal trajectory." For this trajectory the exact operating mode was specified. The pilots then tried flying trajectories which were different from the "nominal" and for which no operating procedure was specified.

The results of the investigation showed that the pilots soon became adept at flying the simulator and could consistently establish orbits lying within an altitude range from 10 to 90 miles. The indicated fuel consumption generally was about 1 to 3 percent of the initial vehicle mass more than that required by use of a two-impulse Hohmann maneuver. The use of the hodograph as a primary display was very effective and could be used to provide much useful information.

INTRODUCTION

Various time tables of space exploration have been proposed as a result of increasing national interest in the conquest of space. Among the many missions in these time tables is exploration of the moon, which, according to most proposed programs, is expected to occur in the foreseeable future. Some of the more interesting problems of the various

proposed lunar missions are those associated with control of a lunar vehicle in the terminal phase. Such problems include guiding the vehicle to a soft landing on the surface, the establishment of a close circular orbit, and a close-approach circumlunar flight. Most of the literature available on studies of these problems consider unmanned automatic-control vehicles or are limited to qualitative analyses or point-mass vehicles. (See refs. 1 to 4.)

Fully automatic control systems require instrumentation to (a) measure the vehicle velocity and position, (b) compare (a) with nominal values, (c) determine if corrective control is required and desirable, and (d) apply corrective control if this action is desired. Acceptable mechanization with respect to accuracy and reliability to perform all these tasks can be expensive in terms of weight and time for component development as well as actual dollar cost. Since man is expected to participate in lunar missions, at least as an observer, it is important to determine if a human, with his inherent ability to compare, reach decisions, and to act, could satisfactorily perform some of the duties just listed for a basic task involved in lunar missions. The basic task selected for this study was the establishment of a close circular lunar orbit; this task was performed on a fixed-base analog simulator. It is assumed that the vehicle has been injected toward the moon and that the ballistic trajectory will result in a near miss with the lunar surface. At the point of closest approach the vehicle velocity would be excessive for capture by the moon. The pilot's task, therefore, is to apply retrothrust in such a manner as to make the point of closest approach occur at an altitude of about 50 miles and simultaneously to reduce the velocity to the value consistent with circular orbital velocity at that altitude.

L 1523

SYMBOLS

E	total energy per unit mass (neglecting rotational energy about body axes), ft^2/sec^2
g_e	gravity at earth's surface, 32.2 ft/sec^2
g_m	gravity at lunar surface, 5.32 ft/sec^2
h	altitude above lunar surface, ft
I_s	specific impulse of rocket, 300 sec
I_X, I_Y, I_Z	moments of inertia about body X-, Y-, and Z-axes, respectively, (note $I_Y = I_Z$), slug-ft^2

M_X, M_Y, M_Z control moments exerted about body X-, Y-, and Z-axes, respectively, ft-lb

m vehicle mass, slugs

m_o initial vehicle mass approaching moon, slugs

$\dot{m}$ time rate of fuel consumption (negative when fuel is being consumed), slugs/sec

L L angular momentum per unit vehicle mass, ft^2/sec

1
5
2
3

l vertical displacement of rocket thrust vector, positive in positive Z-direction, ft

p, q, r rates of rotation about body X-, Y-, and Z-axes, respectively, radians/sec

R radial distance from moon's center, ft

R_m radius of moon, 5.702×10^6 ft

$\dot{R}$ vehicle velocity component in the radial direction, ft/sec

$R\dot{\theta}$ vehicle velocity component in circumferential direction, ft/sec

T rocket thrust along body X-axis, positive in the -X direction, lb

t time, sec

u, v, w vehicle velocities along body X-, Y-, and Z-axes, respectively, ft/sec

$V = \sqrt{u^2 + v^2 + w^2}$

X, Y, Z right-hand body-axis-system coordinates with origin located at vehicle instantaneous center of gravity

X_g, Y_g, Z_g direction cosines between local vertical and body X-, Y-, and Z-axes, respectively

x_i, y_i, z_i right-hand inertial-axis-system coordinates with origin located at center of moon

x, y, z distances along x_i, y_i, and z_i axes, respectively, ft

x', y', z' reference axes parallel to inertial axes

α angular orientation of vehicle in pitch defined as the angle between the projection of the local vertical in body XZ-plane, and the body Z-axis, radians or deg

δ_t rocket throttle control displacement, ft

$\delta_X, \delta_Y, \delta_Z$ hand-controller angular displacements about X-, Y-, and Z-axes, respectively, deg

$\overline{\phi}$ angular orientation of vehicle, defined as the angle between body XZ-plane and local vertical and referred to as bank angle, radians or deg

ψ, θ, ϕ Euler angles of rotation (order of rotation ψ, θ, ϕ), radians or deg

$\overline{\psi}$ angular orientation of vehicle defined as $\frac{v}{\sqrt{u^2 + v^2 + w^2}}$ and referred to as azimuth angle, radians or deg

Subscripts:

a apocynthion conditions

p pericynthion conditions

A dot over a symbol indicates a derivative with respect to time.

EQUATIONS OF MOTION

The basic equations of motion and the auxiliary equations used in this investigation are given in appendix A. These equations were solved on an electronic analog computer operating in real time. There were six basic equations permitting three translatory and three rotational degrees of freedom of the vehicle about its three body axes. The pilot closed the control loop and had direct input into the longitudinal force equation and the three moment equations. A schematic diagram of the equations of motion is presented in figure 1.

The inertial reference frame for these equations was a fixed axis system with its origin located at the center of the moon (fig. 2). The moon was assumed to be a nonrotating homogeneous sphere having a radius of 5.702×10^6 feet and a surface gravity of 5.32 feet per second per second.

L 1523

Vehicle mass and moments of inertia were varied as thrust was applied to account for mass reduction during thrusting. Mass changes due to the use of the moment reaction control jets were not accounted for in the equations of motion since they were negligibly small in comparison with the mass change associated with thrust application.

VEHICLE DESCRIPTION

The vehicle assumed in this study was a body of revolution having the guidance section at the nose, followed by the crew compartment, fuel tankage, and finally the primary thrust nozzle (fig. 3). The thrust was assumed to act along the longitudinal axis of the vehicle and to be variable from zero to its maximum value. As will be pointed out in a subsequent section this variable feature generally was not used; thrust was either applied at maximum level or was completely off. The maximum thrust level chosen for this study resulted in a longitudinal acceleration at initial thrust application of about 0.26 earth g unit or 1.57 lunar g units. Upon orbit attainment, corresponding values of about 0.36 earth g unit and 2.16 lunar g units were obtained as a result of the reduction in vehicle mass. These relatively low values of thrust were selected to simplify the pilot's task and also because the results of reference 5 indicated that there was very little to be gained in terms of fuel efficiency by the use of higher thrust for this maneuver.

Control moments were generated about all three body axes by simulated pairs of reaction jets which applied pure torques. A description of the moment controller is given in the next section, and pertinent vehicle characteristics are given in figure 3.

COCKPIT AND CONTROLS

The general layout of the cockpit may be seen in the photograph presented as figure 4, which shows the relative position of the pilot's chair with respect to the instrument display and controls.

Vehicle thrust was commanded through the use of a simple displacement throttle control located to the left of the pilot. Thrust varied linearly with control displacement.

Moment control about the three body axes was commanded by the pilot through the use of a three-axis hand controller similar to the one that will be used in Project Mercury. This controller was designed to be operated by angular motions of the pilot's right hand about axes passing

through the wrist for pitch, parallel to and slightly below the forearm for roll, and through the longitudinal axis of the grip for yaw (fig. 5(a)). It has maximum angular displacements about each of the three axes of approximately $\pm 15^{\circ}$. During most of the investigation the three-axis controller was used; however, for some flights an optional arrangement consisting of the hand controller for pitch and roll control and a conventional set of rudder pedals for yaw control was used. The control torque commanded by the pilot was proportional to control deflection except for a small dead band that was used for control centering (fig. 5(b)).

INSTRUMENT DISPLAY

Display and controller motions were consistent with the pilot facing in the direction of the rocket nozzle which is also the direction of flight (fig. 2(b)). The information displayed to the pilot included vehicle pitch attitude with respect to the local horizon (α), the vehicle bank attitude ($\bar{\phi}$), yaw or azimuth attitude with respect to the plane of the instantaneous velocity vector ($\bar{\psi}$), angular rates about each of the three body axes, (p, q, and r), altitude ($R - R_m$), radial velocity ($\dot{R}$), and the vehicle circumferential velocity component ($R\dot{\theta}$).

A photograph of the instrument panel is presented as figure 6. The altimeter and the rate-of-descent meters were three-hand dial instruments. Angular rates about each of the three body axes were presented on a single instrument that contained three needle indicators, each of which moved in translation. Pitch rate was provided by the needle that translates up and down. Yaw and roll rates were given by needles translating from left to right.

Located to the pilot's left, above the throttle, was a single-channel conventional two-variable plotter (fig. 4) that presented a continuous trace of the vehicle circumferential velocity component $R\dot{\theta}$ plotted against the radial velocity component $\dot{R}$. This chart was used as the primary source for information regarding piloting technique. Information other than the vehicle velocity components could be presented on the chart. This information and some of its potential uses are discussed in appendix B.

Although the radial velocity component $\dot{R}$ was presented in two places - on a dial and also on the plotter - the dial instrument was used when making fine adjustments because of the accuracy with which it could be read.

LUNAR APPROACH BALLISTIC TRAJECTORIES

Two primary factors were considered in selecting a basic approach trajectory. First, the trajectory should be one which could be obtained either by direct earth launch with little or no corrections after injection or by departure from an earth orbit. Second, a relatively simple guidance and control scheme should be sufficient to place the vehicle in the desired lunar orbit. On the basis of these two factors, one "nominal" trajectory was determined. This would then be the trajectory which the vehicle would follow if injected perfectly. Since perfect injection is unattainable in practice, there would exist certain errors from the nominal trajectory. The vehicle would then follow some off-nominal trajectory. In this study one nominal and several off-nominal trajectories were selected. These are described in more detail as follows.

Nominal Trajectory

The nominal trajectory selected was one which would have a miss distance of 294,000 feet above the lunar surface and a velocity of 8,466 feet per second at this point. This trajectory is one of the three-dimensional trajectories used in the error analysis of reference 6 for injection conditions of 300 miles altitude and a velocity of 35,131 feet per second; this trajectory also fits the first requirement stated previously. The trajectory could be modified to result in a circular lunar orbit by applying a constant thrust in the plane of the velocity vector and normal to the local vertical ($\alpha = 0^{\circ}$); hence, the second requirement would be met. The required thrust level resulted in an initial deceleration of 0.26 earth g unit and had to be applied when the altitude above the lunar surface was 383,700 feet and terminated at an altitude of 264,000 feet. A sketch of the trajectory relative to the moon is presented in figure 7.

Off-Nominal Trajectories

The off-nominal trajectories had certain characteristics different from the nominal trajectory, such as might be expected from small errors in injection conditions or residual errors after midcourse corrections. The off-nominal trajectories were specified by imposing velocity increments of ±200 feet per second on the radial and circumferential velocity components and by increments of ±100,000 feet in altitude from the values of the nominal trajectory at the time of problem initiation. Since the terminal phase was the region of interest in this investigation, the problem was initiated in the vicinity of 1,000,000 feet altitude. The

following table shows the initial conditions and combination of miss distance and velocity for the various trajectories:

Initial conditions			Pericynthion		Remarks
Radial velocity, ft/sec	Circumferential velocity, $R\dot{\theta}$, ft/sec	Altitude, h, ft	Altitude, h, ft	Circumferential velocity, $R\dot{\theta}$, ft/sec	
-2,867	7,575	1,000,000	294,800	8,466	Nominal trajectory
-2,867	7,775	1,000,000	342,600	8,617	High in initial $R\dot{\theta}$
-2,867	7,375	1,000,000	238,600	8,320	Low in initial $R\dot{\theta}$
-3,067	7,575	1,000,000	213,700	8,582	High in initial $-\dot{R}$
-3,067	7,775	1,000,000	267,800	8,729	High in initial $-\dot{R}$ and $R\dot{\theta}$
-3,067	7,375	1,000,000	153,100	8,442	High in initial $-\dot{R}$; low in $R\dot{\theta}$
-2,667	7,575	1,000,000	374,100	8,355	Low in initial $-\dot{R}$
-2,667	7,775	1,000,000	419,600	8,512	Low in initial $-\dot{R}$; high in $R\dot{\theta}$
-2,667	7,375	1,000,000	322,800	8,203	Low in initial $-\dot{R}$; low in $R\dot{\theta}$
-2,867	7,575	900,000	198,900	8,475	Low in altitude
-2,867	7,575	1,100,000	390,500	8,457	High in altitude

This range of initial conditions results in a corridor (at pericynthion) of about 50 miles for the ballistic trajectory of the vehicle.

PILOT'S TASK AND PROCEDURE

As indicated previously, the pilot's task was that of establishing a circular orbit at an altitude of 50 miles (264,000 feet) above the lunar surface. This amounts to modifying the terminal phase of the ballistic trajectory so as to reduce the vehicle velocity components to $\dot{R} = 0$ and $R\dot{\theta} = 5{,}385$ ft/sec at an altitude of 264,000 feet. The procedure to accomplish this task involved the following steps:

(a) Obtain a zero bank-angle attitude.

(b) Aline the vehicle thrust axis (body axis) in the plane of the trajectory.

(c) Pitch the vehicle to the desired attitude.

(d) Apply thrust.

(e) Maintain proper vehicle attitude and thrust to approach the desired orbit conditions.

(f) Terminate thrust when the desired orbit conditions are attained.

A reasonable approach in accomplishing these tasks would be to determine first the local vertical and aline the vehicle vertical (Z) axis with the local vertical (possibly by use of horizon scanners); this accomplishes step (a). The next step would be to view the lunar surface through a telescope with objective lens parallel to the vehicle Z-axis and with the objective lens gridded with lines parallel to the vehicle X-axis. Observation of motion of the lunar surface at an angle relative to the grid lines would indicate that the vehicle was yawed with respect to the plane of the trajectory; hence, the vehicle could be yawed to the proper direction. Thus, step (b) could be accomplished. Step (c) could be accomplished by then measuring the displacement of the vehicle Z-axis relative to the local vertical. The pitch attitude required during thrust is a function of the altitude and velocity components and is part of the guidance scheme. The technique used by the pilot in monitoring the pitch angle α depends on the trajectory and on his judgment. As stated in the section entitled "Lunar Approach Ballistic Trajectories," the nominal trajectory could be handled by maintaining α at zero degrees from thrust application (at 383,700 feet altitude) until the desired altitude was reached. The procedure in flying off-nominal trajectories involved proper monitoring of α and was left to the discretion of the pilot.

L 1523

The method of determining vehicle orientation as just outlined is one which might be applicable in flight or on a simulator with visual projection of the lunar surface and could of course be replaced by other more sophisticated schemes. In the present investigation the attitude angles were computed and presented on various meters. It should be noted that if thrust were applied with the thrust vector not in the trajectory plane, the vehicle would move into a new trajectory plane, and the display instruments would indicate vehicle attitude angles relative to the new plane. No instrument display was provided to enable the pilot to acquire the original approach trajectory plane since this was not felt to be an important phase of the present study. Such a display could, of course, have been provided.

PRELIMINARY COMPUTATIONS

Nominal Trajectory

The primary guidance for the pilot was supplied as a hodograph of the velocity components $\dot{R}$ and $R\dot{\theta}$ for a precise nominal trajectory.

This trajectory was computed on an electronic data processing machine and was traced on the two-variable plotter (fig. 4) prior to piloted flights. The altitude for a number of points on this trace also was indicated. Figure 8 shows the hodograph of the nominal trajectory. The fuel consumption computed for this maneuver was 27.7 percent of the initial vehicle mass and was obtained for the assumed initial acceleration value of 0.26 earth g unit and specific impulse of 300 seconds. As a matter of interest, a two-impulse maneuver utilizing a Hohmann transfer ellipse would require fuel consumption of 27.6 percent of the initial mass. The difference of about 0.1 percent of the vehicle mass is a measure of the penalty of utilizing the finite thrust level chosen for the nominal trajectory.

L
1
5
2
3

Target Area in the Hodograph Plane

The precise accomplishment of the piloting task required the simultaneous achievement of the specific values $\dot{R} = 0$, $R\dot{\theta} = 5{,}385$, and $h = 264{,}000$ feet. The results of a few piloted flights on the simulator showed that such a degree of proficiency would be very difficult to attain and that some error in each of these parameters would be inevitable. Because of this, it was decided that the pilot should try to terminate thrust for any combination of conditions which would establish an orbit having a maximum apocynthion of 90 miles above the lunar surface, and a minimum pericynthion of 10 miles above the lunar surface. Preliminary flights on the simulator showed that thrust generally was terminated in the altitude range from 240,000 feet to 288,000 feet. A hodograph target area therefore was specified by computing the range of velocities which would be acceptable at each of these altitudes to yield the permissible apocynthion and pericynthion boundaries. The target in the hodograph plane under the conditions given can be found from the following considerations. After thrust termination the vehicle is again in a free ballistic trajectory with constant energy and angular momentum; hence,

$$\frac{1}{2}\left[\dot{R}^2 + \left(R\dot{\theta}\right)^2\right] - g_m\left(\frac{R_m^2}{R}\right) = E = \text{Constant} \tag{1}$$

and

$$R^2\dot{\theta} = L = \text{Constant} \tag{2}$$

From equation (1),

$$\dot{R}^2 + \left(R\dot{\theta}\right)^2 - 2g_m\left(\frac{R_m^2}{R}\right) = \left(R\dot{\theta}\right)_a^2 - 2g_m\left(\frac{R_m^2}{R_a}\right) \tag{3}$$

From equation (2),

$$R^4\dot{\theta}^2 = R_a^2\left(R\dot{\theta}\right)_a^2 \tag{4}$$

Substituting equation (4) into equation (3) gives

$$\dot{R}^2 + \left[\left(R\dot{\theta}\right)^2\right]\left[1 - \frac{R^2}{(R_a)^2}\right] = -2g_m R_m^2\left(\frac{1}{R_a} - \frac{1}{R}\right) \tag{5}$$

For given values of R and R_a, equation (5) specifies an ellipse since R is less than R_a. A similar relationship holds for R_p, but the equation then specifies a hyperbola since R is greater than R_p. For each value of R, there is obtained an area enclosed by an ellipse on one side and a hyperbola on the other. For the two values selected, 5,942,000 and 5,990,000 feet corresponding to altitudes of 240,000 feet and 288,000 feet, respectively, two closed curves are obtained (fig. 9). The region (area) common to both sets of closed curves then specifies the combinations of $\dot{R}$ and $R\dot{\theta}$ which must be attained within the altitude range from 240,000 to 288,000 feet at thrust termination in order that the vehicle orbit have a minimum pericynthion of 10 miles and a maximum apocynthion of 90 miles.

RESULTS AND DISCUSSION

All results presented in this paper were obtained with the authors as the "pilots." However, a number of other subjects, including two men with considerable military flying experience and some simulator work, flew the simulator, and their opinion tempered the following discussion. The results of the present investigation can be divided conveniently into two groups, one dealing with the nominal trajectory and the other, with the off-nominal trajectories. This division is a logical one since the piloting technique was specified exactly for the nominal trajectories but not for the off-nominal trajectories.

Nominal Trajectory

This trajectory was used primarily for familiarizing the pilots with the instrument display, controls, and indicated dynamics of the vehicle. The problem was initiated at an altitude of about 1×10^6 feet with the vehicle alined with the velocity vector. This condition resulted in a value of α of -20°. The pilot was not required to have

the vehicle properly oriented for thrust application until it reached an altitude of 383,700 feet; therefore, he had several minutes available to reduce α to zero before applying thrust. Since the equations of motion are for a spherical moon, α will move toward zero as the vehicle proceeds along the ballistic flight path. Consequently, the pilot, by taking advantage of this fact, could reduce the amount of control fuel needed. Similarly, the apparent pitch rotation of the vehicle indicated by the α meter requires the pilot to introduce a small pitch rate in order to maintain α at zero for the controlled portion of the trajectory.

The calculated nominal ballistic and controlled trajectories were traced on the hodograph for pilot guidance prior to each flight. With a little practice to establish a feel for the geometry of the problem and the dynamics of the vehicle, the pilots had no difficulty in flying the nominal trajectory. The results of a typical flight are shown in figure 10 and indicate the establishment of an orbit reasonably close to the desired orbit. The difference between the calculated and the computed ballistic trajectories (before any thrust was applied) is caused by computer drift. The initial conditions for the analog were biased a small amount to minimize this difference over the no-thrust portion of the trajectory.

L 1 5 2 3

Flights starting at an altitude of 1×10^6 feet required about 11 to 12 minutes real time to complete. Approximately one-half of this time was spent in the ballistic trajectory approaching thrust initiation altitude, and the remaining half, in the controlled trajectory portion. For the flight shown in figure 10 the amount of fuel expended during the controlled portion of the trajectory represented 29.2 percent of the initial vehicle mass. Digital calculations indicated that 27.7 percent should be required to perform the maneuver. A number of piloted flights of this nominal trajectory were made (about ten flights) and, in general, the indicated amount of fuel expended was of the order of 1 to $1\frac{1}{2}$ percent of the initial vehicle mass greater than the results from digital computations. However, due to the length of time required for these flights and the range of the variables involved, it was determined that this difference was bordering on the accuracy of the analog computations. The pilots had no difficulty in maintaining proper vehicle alinement throughout the trajectory or in applying thrust at the proper altitude and, hence, the fuel consumption should be very close to the value obtained from the digital computations.

The indicated altitude at thrust termination of the piloted nominal trajectories was consistently lower than the altitude obtained from the digital computations when the pilot attempted to trace the hodograph path closely. This was attributed to a combination of the long running time and the distance scaling required for the analog computer in this

problem. When the pilot attempted to terminate thrust at the proper altitude, he was required to depart from the $\alpha = 0$ thrust procedure.

Off-Nominal Trajectories

There were two regions of interest in working with the off-nominal trajectories. One was the determination of the pattern of logic and technique which evolved for monitoring the vehicle pitch angle α, and the other was measurement of the pilot proficiency in establishing an acceptable orbit.

L
1
5
2
3

Piloting logic and technique. - There were a few obvious guidelines which could be used by the pilots in performing their task. It is apparent that in order to reach $\dot{R} = 0$ and $R\dot{\theta} = 5,385$ it is necessary to reduce the values of these parameters by the increments

$$\Delta\dot{R} = \dot{R}$$

$$\Delta R\dot{\theta} = R\dot{\theta} - 5,385$$

In order to reduce both increments to zero simultaneously, it would appear that the vehicle pitch angle α should be adjusted to the value

$$\tan \alpha = \frac{\Delta\dot{R}}{\Delta R\dot{\theta}}$$

This equation, however, does not take into account the altitude at which the desired velocities are attained, and hence the attitude angle must be modified to account for altitude differences between piloted and nominal trajectories. This additional factor can be rationalized on the basis that a positive value of α is required to increase the rate of descent, and a negative value of α is required to reduce the rate of descent. The attitude equation, therefore, is of the form

$$\tan \alpha = f\left[\left(\frac{\Delta\dot{R}}{\Delta R\dot{\theta}}\right), \quad \left(h - h_{nominal}\right)\right]$$

No attempt was made to define exactly the functions f. Actually, the pilots were supplying this function as they flew the simulator.

With these basic considerations, a piloting technique evolved which can be described in terms of the vehicle hodograph trace. The vehicle generally was permitted to proceed along its uncontrolled ballistic

trajectory while the pilot visually compared its hodograph trace with the trace of the nominal trajectory. As the vehicle trace approached the vicinity of the point of thrust application of the nominal trajectory (h = 383,700 feet) the pilot would check the altitude. If the altitude above the lunar surface was in excess of about 384,000 feet he would pitch the vehicle rocket upward (positive α) and apply thrust to make $\dot{R}$ more negative. If the altitude was less than about 384,000 feet he would make α negative and apply thrust to make $\dot{R}$ less negative (reduce the rate of descent). The magnitude of α was varied during the thrusting operation to attempt to make the vehicle follow the nominal hodograph. However, excursions were made from the hodograph as might be required to correct the altitude. In some instances it became apparent that the vehicle attitude was not particularly suited for continuation of thrust. Because of the low torques assumed for this vehicle, the pilots found it expedient to terminate thrust, reorient the vehicle, and then apply thrust. It soon became evident that the pilots were not utilizing the variable-thrust feature, but instead were using the throttle as a simple on-off type of control.

L 1 5 2 3

The pertinent results of several pilot-controlled flights are given in figures 11 to 13. These are typical of a large number of flights and are described in some detail to clarify the piloting technique. The pilot was not told beforehand what the initial conditions would be for each problem, and hence could not plan his procedure before the flight. His decisions on procedure were based entirely on observation of the display panels and the general logic outlined in the preceding paragraph.

Figure 11 shows the results of a flight having an initial altitude of 1×10^6 feet, a circumferential velocity component $R\dot{\theta}$ of 7,575 feet per second, and a rate of descent $\dot{R}$ of -3,067 feet per second, which is a rate of descent 200 feet per second greater than for the nominal case. The results show that the pilot permitted the vehicle to follow a ballistic path and observed that for his altitude the vehicle rate of descent was higher than that of the nominal trajectory. In order to reduce the rate of descent, thrust had to be applied with the rocket nozzle tilted downward (negative α). Therefore, the pilot chose to rotate the vehicle to $\alpha = -20^\circ$, and at an altitude of 300,000 feet, applied full thrust. The hodograph trace shows that the rate of descent was reduced fairly rapidly; however, the vehicle altitude was below the desired altitude when the rate of descent was stopped. Since the circumferential velocity $R\dot{\theta}$ was in excess of circular orbital speed, the vehicle began to climb. The pilot therefore rotated the vehicle to thrust only against $R\dot{\theta}$ ($\alpha = 0$). The vehicle then lost circumferential velocity more rapidly, but continued to climb because of the centrifugal acceleration. In order to prevent the vehicle from climbing to an excessive altitude, the pilot rotated the vehicle to positive values

of α to force $\dot{R}$ toward zero. The hodograph trace shows that the pilot succeeded in passing through the hodograph target area. Another flight (fig. 12) with the same initial conditions was attempted; however, in this case the pilot started thrust application at a higher altitude (400,000 feet). The end results are the same as those of figure 11.

In the flights of figures 11 and 12 the pilot chose to maintain full thrust from thrust initiation until the vehicle passed through the target in the hodograph. In other flights, conditions occurred which made it desirable to terminate thrust before attaining the target; the vehicle was then permitted to follow a new ballistic trajectory for a short period. After this, thrust was applied again to establish the desired orbit. Such a case is shown in figure 13. The initial conditions were an altitude of 1×10^6 feet and velocity components $\dot{R} = -2{,}667$ and $R\dot{\theta} = 7{,}575$ (rate of descent 200 feet per second less than nominal). The vehicle attitude during the early part of the thrust period can be rationalized in terms of vehicle altitude and velocity as previously discussed. Near the target, however, the vehicle was still too high. The pilot therefore terminated the thrust and permitted the vehicle to approach the nominal trajectory on a ballistic path. Physically, the vehicle was on the approach phase of its trajectory and therefore was losing altitude. When the altitude was close to that desired, the pilot applied thrust to obtain the desired orbit velocity.

The only factor in the control of the vehicle which was confusing to various pilots who volunteered to fly the simulator was associated with the effects of centrifugal acceleration on the motion of the lunar vehicle. On familiarization flights the tendency was to thrust against $R\dot{\theta}$ and permit $\dot{R}$ to go to zero as it normally would, since the vehicle was approaching pericynthion. As $\dot{R}$ reached zero, the new pilots failed to realize that $\dot{R}$ would now become positive even with no applied thrust, and hence became confused when R began to increase in magnitude quite rapidly. This matter was generally cleared up by consideration of the dynamics of the motion involved. After a few practice flights new pilots had little or no difficulty in flying the simulator and even used the effects of centrifugal acceleration to advantage in obtaining altitude changes.

Pilot proficiency. - It is not feasible at this stage to measure pilot proficiency on an absolute basis in terms of fuel consumption because the path and thrust program for minimum fuel consumption between initial conditions and the desired final (end) conditions was not defined. The basis for judging pilot proficiency therefore was (a) how well he accomplished his task based on achieving the desired end conditions, and (b) how much fuel was used and how this compared with a

computed two-impulse maneuver (Hohmann transfer). The results for such comparisons for several off-nominal cases are presented in figure 14. It should be noted that a number of flights were made for each of the sets of initial conditions previously tabulated. The results of figure 14 are, however, considered representative of all the data obtained. In all cases the flights were terminated in the hodograph target area within the altitude range from 240,000 to 288,000 feet. The target defines all trajectories having a minimum pericynthion of 10 miles and a maximum apocynthion of 90 miles.

The fuel consumption for the various off-nominal trajectories is shown in figure 14 and indicates that from 27.5 to 31.2 percent of the initial vehicle mass was used to establish the desired orbit. This range is from 1 to 3 percent more fuel than required for a computed two-impulse Hohmann transfer, where the initial impulse is applied at the pericynthion of the approach ballistic trajectory. The fuel consumption of the piloted flights could have been made to approach that of the Hohmann transfer by applying thrust for short periods as the vehicle passed through pericynthion on each orbit and by taking several orbits to brake from hyperbolic speed to circular speed at an altitude of 50 miles. This technique is time consuming and was not considered in the present investigation.

L
1
5
2
3

SUPPLEMENTARY INVESTIGATIONS

During the present investigation it was deemed advisable to explore briefly certain factors which were related to the basic problem. These were (a) the effects of thrust misalinement, (b) the use of another type of moment control system, and (c) the use of a modified display panel.

Thrust misalinement.- A thrust misalinement was introduced into the pitching-moment equation so that a pitchup was introduced with thrust application. With full thrust, the pitching moment was about one-quarter of that available from the pitch controller and corresponded to about 0.1° of rocket-nozzle misalinement. Flights made with thrust misalinement present were initially somewhat more difficult than those with no misalinement. The difficulty was associated with two factors: (1) With thrust on, it was difficult to hold the controller at exactly the correct position to eliminate the unwanted pitching moment, and (2) the pilot sometimes inadvertently neglected the α meter for a short time and thus permitted the pitching moment to become unbalanced. This led to large excursions from the desired pitch angle. With a small amount of practice, however, the pilots could control the thrust misalinement with little difficulty.

Moment controller.- The controller used in most of the investigation reported herein was a three-axis hand controller. (See fig. 5.) In previous investigations (refs. 7 and 8, for example) some pilots had indicated a preference for a two-axis hand controller (pitch and roll) and a set of rudder pedals (yaw control). In order to get a comparison of both systems, the yaw axis of the three-axis controller was locked and a set of rudder pedals installed for yawing-moment application. Both authors of this paper made several flights using the rudder-pedal controls. For this particular combination of low torque-to-inertia ratios and reasonably small vehicle angular displacements, both pilots preferred the three-axis hand controller over the combination of a two-axis controller and rudder pedals. It was felt that the leg motions required for rudder control resulted in coarse control in comparison with that obtainable with the hand controller. Treadle foot pedals might have eliminated this unfavorable comparison. Results of other investigations (refs. 7 and 8) have indicated that when high angular rates and displacements are encountered, a two-axis hand controller and foot pedals have an advantage in permitting more precise application of combined control.

Instrument display.- Most of this investigation was made with the display shown in figure 4. This display was felt to be adequate and permitted the pilot to perform the desired task with good proficiency. A few flights were made with a "two-axis eight-ball" replacing the α and ϕ meters. The authors made several flights with the eight-ball as part of the display. The feeling was that this reduced the scanning problem slightly but did not provide the accuracy available with the linear α and ϕ meters. Since the scanning problem was not critical because of the relatively slow motions involved and since angular positions (particularly α) were quite important, the authors preferred the linear meters over the eight-ball. For problems requiring rapid scanning an eight-ball probably would be preferred.

Some attempts were made to use the hodograph as an indicator of $\dot{R}$ and $R\dot{\theta}$, without actually tracing out the instantaneous values of these velocities. This was felt to be comparable to having a display of $\dot{R}$ and $R\dot{\theta}$ on meters. These attempts showed that the slope of the $\dot{R}$, $R\dot{\theta}$ trace was important to the pilot in establishing the desired pitch angle.

CONCLUDING REMARKS

A study has been made on a six-degree-of-freedom fixed-base simulator of the ability of human pilots to modify ballistic trajectories of a space vehicle approaching the moon to establish a circular orbit

about 50 miles above the lunar surface. The unmodified ballistic trajectories had miss distances from the lunar surface of from 40 to 80 miles and a velocity range of from 8,200 to 8,700 feet per second at closest approach. The pilot was given control of the thrust (along the vehicle longitudinal axis) and torques about all three body axes. The information display given to the pilot was a hodograph of the vehicle rate of descent and circumferential velocity, an altimeter, and vehicle attitude and rate meters.

The general procedure used in the investigation was to permit the pilots to become familiar with the instrumentation, controls, and indicated vehicle dynamics by flying a simple nominal trajectory. For this trajectory the exact operating mode was specified. The pilots then tried flying trajectories which were different from the nominal and for which no operating procedure was specified.

L
1
5
2
3

The results of the investigation showed that the pilots soon became adept at flying the simulator and could consistently establish orbits lying within an altitude range from 10 to 90 miles. The indicated fuel consumption generally was about 1 to 3 percent of the initial vehicle mass more than that required by use of a two-impulse Hohmann maneuver. The use of the hodograph as a primary display was very effective and could be used to provide much useful information.

Langley Research Center,
National Aeronautics and Space Administration,
Langley Field, Va., April 26, 1961.

APPENDIX A

EQUATIONS OF MOTION

The six equations of motion of the vehicle represent the three translational and three rotational degrees of freedom about the vehicle principal axes. The inertial reference axis system has its origin at the center of the moon (fig. 2(a)). A spherically symmetric gravitational field about the moon was assumed. The force equations used are as follows:

L
1
5
2
3

X-direction,

$$\dot{u} + qw - rv = -\frac{T}{m} - g_m X_g \left(\frac{R_m}{R}\right)^2 \tag{A1}$$

Y-direction,

$$\dot{v} + ru - pw = -g_m Y_g \left(\frac{R_m}{R}\right)^2 \tag{A2}$$

Z-direction,

$$\dot{w} + pv - qu = -g_m Z_g \left(\frac{R_m}{R}\right)^2 \tag{A3}$$

The vehicle considered in this investigation had thrusting capability only in the direction of the vehicle's longitudinal axis. Figure 2(b) shows the orientation of the vehicle with respect to the body-axis system used.

The moment equations, which assume rigid-body dynamics, are as follows:

rolling moment,

$$\dot{p} + p\frac{\dot{I}_X}{I_X} = \frac{M_X}{I_X} \tag{A4}$$

pitching moment,

$$\dot{q} + pr\frac{(I_X - I_Y)}{I_Y} + q\frac{\dot{I}_Y}{I_Y} = \frac{M_Y}{I_Y} + \frac{Tl}{I_Y} \tag{A5}$$

yawing moment,

$$\dot{r} + pq \frac{(I_Y - I_X)}{I_Y} + \frac{r\dot{I}_Y}{I_Y} = \frac{M_Z}{I_Y} \tag{A6}$$

The terms M_X, M_Y, and M_Z are control moments which were generated about the three axes by assumed reaction jets that were considered to operate in pairs so as to apply pure torques about each axis. A limited number of flights were made with the inclusion of the thrust misalinement term Tl in the pitch equation.

The moment equations, as presented, are written about the vehicle center of gravity which was located on the vehicle longitudinal axis. It should be noted that mass reduction, as a result of thrusting, causes movement of the center of gravity along the X-axis and, of course, changes the vehicle's moments of inertia. Also, since the vehicle was considered to be a body of revolution, I_Z and $\dot{I}_Z$ were assumed to be equal to I_Y and $\dot{I}_Y$.

In addition to the six equations of motion, a number of auxiliary equations were employed. The auxiliary equations are as follows:

$$\dot{\psi} = r \frac{\cos \phi}{\cos \theta} + q \frac{\sin \phi}{\cos \theta} \tag{A7}$$

$$\dot{\theta} = q \cos \phi - r \sin \phi \tag{A8}$$

$$\dot{\phi} = p + q \tan \theta \sin \phi + r \tan \theta \cos \phi \tag{A9}$$

$$X_g = \frac{x}{R} \cos \psi \cos \theta + \frac{y}{R} \sin \psi \cos \theta - \frac{z}{R} \sin \theta \tag{A10}$$

$$Y_g = \frac{x}{R}(\cos \psi \sin \theta \sin \phi - \sin \psi \cos \phi) + \frac{y}{R}(\sin \psi \sin \theta \sin \phi + \cos \psi \cos \phi) + \frac{z}{R} \cos \theta \sin \phi \tag{A11}$$

$$Z_g = \frac{x}{R}(\cos \psi \sin \theta \cos \phi + \sin \psi \sin \phi) + \frac{y}{R}(\sin \psi \sin \theta \cos \phi - \cos \psi \sin \phi) + \frac{z}{R} \cos \theta \cos \phi \tag{A12}$$

L 1523

$$\dot{x} = u \cos \psi \cos \theta + v(\cos \psi \sin \theta \sin \phi - \sin \psi \cos \phi) + w(\cos \psi \sin \theta \cos \phi + \sin \psi \sin \phi) \tag{A13}$$

$$\dot{y} = u \sin \psi \cos \theta + v(\sin \psi \sin \theta \sin \phi + \cos \psi \cos \phi) + w(\sin \psi \sin \theta \cos \phi - \cos \psi \sin \phi) \tag{A14}$$

$$\dot{z} = -u \sin \theta + v \cos \theta \sin \phi + w \cos \theta \cos \phi \tag{A15}$$

L
1
5
2
3

$$\dot{R} = \frac{x\dot{x} + y\dot{y} + z\dot{z}}{R} \tag{A16}$$

$$R = \sqrt{x^2 + y^2 + z^2} \tag{A17}$$

$$R\dot{\theta} = \sqrt{\dot{x}^2 + \dot{y}^2 + \dot{z}^2 - \dot{R}^2} = \sqrt{u^2 + v^2 + w^2 - \dot{R}^2} \tag{A18}$$

$$m = m_o + \int \dot{m}\, dt \tag{A19}$$

$$\dot{m} = -\frac{T}{g_e I_s} \tag{A20}$$

The thrust in the X-direction equation and the control torques in the moment equations were the only inputs into the equations of motion of the vehicle that were under the control of the pilot. Since only proportional controls were considered in the investigation, the resulting control functions are expressed in the following manner:

$$T_X = \frac{dT_X}{d\delta_t} \delta_t \tag{A21}$$

$$M_X = \frac{dM_X}{d\delta_X} \delta_X \tag{A22}$$

$$M_Y = \frac{dM_Y}{d\delta_Y} \delta_Y \tag{A23}$$

$$M_Z = \frac{dM_Z}{d\delta_Z}\,\delta_Z \tag{A24}$$

The slopes shown in equations (A21) to (A24) were held constant for the entire investigation. (See fig. 5(b).)

The moments of inertia in equations (A4), (A5), and (A6) were obtained by assuming a weight breakdown for the vehicle which permitted evaluating the moments of inertia as functions of vehicle mass m. Values for $\dot{I}_X$ and $\dot{I}_Y$ were found as follows:

$$\dot{I}_X = \frac{dI_X}{dm}\frac{dm}{dt} = \frac{dI_X}{dm}\,\dot{m} \tag{A25}$$

$$\dot{I}_Y = \frac{dI_Y}{dm}\,\dot{m} \tag{A26}$$

The only additional expressions utilized in the analog program were those associated with the vehicle attitude as presented on the pilot's display panel. The attitude angles were defined as follows:

vehicle pitch attitude,

$$\alpha = \tan^{-1}\frac{X_g}{Z_g}$$

vehicle bank attitude,

$$\bar{\phi} = Y_g$$

vehicle azimuth attitude,

$$\bar{\psi} = \frac{v}{\sqrt{u^2 + v^2 + w^2}}$$

It is apparent that $\bar{\phi}$ is not truly a bank angle nor is $\bar{\psi}$ a true azimuth angle except when both of these angles are small and $\alpha \approx 0$. However, most of the thrusting was anticipated to occur with these angles close to zero. Also, it should be noted that if the vehicle was pitched to large values of α during piloted flight and excursions in $\bar{\phi}$ and $\bar{\psi}$ occurred, the pilot had in effect a cross-control situation wherein application of control in either roll or yaw would change both azimuth and bank angle.

APPENDIX B

GUIDANCE HODOGRAPH

General Discussion

The basic task of the pilot was that of modifying the vehicle velocity and altitude from the ballistic approach trajectory to a circular orbit at an altitude of 50 miles. There was no attempt to select a particular orbit plane. The problem is essentially two dimensional if the pilot maintains proper vehicle orientation. The important parameters for the task are then $\dot{R}$, $R\dot{\theta}$, and h. Several methods were considered for presenting these quantities to the pilot, along with the other variables necessary to maintain proper vehicle attitude. The scheme which appeared to be particularly suited to the problem involved the use of a plotter which traced out the instantaneous values of $\dot{R}$ and $R\dot{\theta}$. This trace, in combination with an altimeter was used to compare the piloted trajectories with a nominal trajectory and indicates what corrective action is required.

The trace of a ballistic trajectory in the hodograph is a circle with the center on the $R\dot{\theta}$-axis as can be seen by examination of the energy and angular momentum equations. The total energy per unit vehicle mass is

$$E = \frac{1}{2}\left[\dot{R}^2 + \left(R\dot{\theta}\right)^2\right] - \frac{g_m R_m^2}{R} = \text{Constant} \tag{B1}$$

The angular momentum per unit mass is

$$L = R\left(R\dot{\theta}\right) = \text{Constant} \tag{B2}$$

Substituting equation (B2) into equation (B1) results in

$$E = \frac{1}{2}\left[\dot{R}^2 + \left(R\dot{\theta}\right)^2\right] - \frac{g_m R_m^2}{L} R\dot{\theta} \tag{B3}$$

or

$$2E + \frac{R_m^4 g_m^2}{L^2} = \dot{R}^2 + \left(R\dot{\theta} - \frac{R_m^2 g_m}{L}\right)^2 \tag{B4}$$

Equation (B4) is the equation of a circle with center at $\dot{R} = 0$, $R\dot{\theta} = \frac{R_m^2 g_m}{L}$ and having a radius of $\left(2E + \frac{R_m^4 g_m^2}{L^2}\right)^{1/2}$. The behavior of the hodograph trace is interesting for the various types of trajectories, that is, for circular, elliptic, parabolic, and hyperbolic orbits. In the case of a circular orbit, $\dot{R}$ is always zero, and there is a balance between the centrifugal and the gravitational forces; hence,

$$\frac{\left(R\dot{\theta}\right)^2}{R} = \frac{g_m R_m^2}{R^2}$$

L
1
5
2
3

therefore,

$$R\dot{\theta} = R_m\sqrt{\frac{g_m}{R}} \qquad \text{(B5)}$$

This is a point on the hodograph and, of course, its position depends only on the specified orbit altitude.

All trajectories have a positive value of the quantity $2E + \frac{R_m^4 g_m^2}{L^2}$ as can be seen from equation (B4). For elliptic trajectories the total energy E is negative, and the hodograph has real intercepts only on the $R\dot{\theta}$ axis at

$$R\dot{\theta} = \frac{R_m^2 g_m}{L} \pm \left(2E + \frac{R_m^4 g_m^2}{L^2}\right)^{1/2}$$

These values represent the apocynthion and pericynthion velocities of the trajectory.

Parabolic trajectories are characterized by having zero total energy. In this case there are intercepts only on the $R\dot{\theta}$ axis, at

$$R\dot{\theta} = 0$$

$$R\dot{\theta} = \frac{2R_m^2 g_m}{L}$$

The value of $\frac{2R_m^2 g_m}{L}$ is, of course, the pericynthion velocity.

Hyperbolic trajectories are characterized by a positive value of total energy E. For such trajectories real intercepts occur on the $\dot{R}$ axis at

$$\dot{R} = \pm(2E)^{1/2}$$

and on the $R\dot{\theta}$ axis at

$$R\dot{\theta} = \left(2E + \frac{R_m^4 g_m^2}{L^2}\right)^{1/2} + \frac{R_m^2 g_m}{L}$$

L
1
5
2
3

The trace for the hyperbolic trajectory is not a closed path, as would be expected from the physical characteristics of such trajectories. Typical traces of the various types of trajectories on the hodograph plane are shown in figure 15.

In the present investigation the task of the pilot was to reach an altitude of 50 miles with certain values of velocity components, $\dot{R} = 0$ and $R\dot{\theta} = 5{,}385$. A plot showing the hodograph traces of a family of trajectories having a 50-mile-altitude pericynthion was therefore determined and is shown in figure 16. These traces were computed by use of equations (B1) and (B2) in the forms

$$E = \frac{1}{2}\left[\dot{R}^2 + \left(R\dot{\theta}\right)^2\right] - \frac{g_m R_m^2}{R}$$

$$= \frac{1}{2}\left(R\dot{\theta}\right)_p^2 - \frac{g_m R_m^2}{R_p} \tag{B6}$$

and

$$L = R\left(R\dot{\theta}\right) = R_p\left(R\dot{\theta}\right)_p \tag{B7}$$

Substituting equation (B7) into equation (B6) yields

$$\frac{1}{2}\left[\dot{R}^2 + \left(R\dot{\theta}\right)^2\right] - \frac{g_m R_m^2}{R_p}\frac{R\dot{\theta}}{\left(R\dot{\theta}\right)_p} = \frac{1}{2}\left(R\dot{\theta}\right)_p^2 - \frac{g_m R_m^2}{R_p} \tag{B8}$$

Equation (B8) specifies $\dot{R}$ and $R\dot{\theta}$ as a function of R_p and $\left(R\dot{\theta}\right)_p$. Constant altitude lines as shown in figure 16 are obtained from equation (B7) by noting that

$$h = R - R_m = R_p \frac{\left(R\dot{\theta}\right)_p}{R\dot{\theta}} - R_m \tag{B9}$$

Therefore, for a given altitude and value of $\left(R\dot{\theta}\right)_p$, the value of $R\dot{\theta}$ is specified. The intersection of the constant-altitude line with the $R\dot{\theta}$-axis shows the apocynthion velocity corresponding to the elliptic orbit having that altitude at apocynthion and a 50-mile pericynthion.

L 1 5 2 3

Various uses of the hodograph are apparent. For example, assume that the lunar vehicle has been launched from earth and its orbital elements indicate a miss distance in the neighborhood of 50 miles at a pericynthion velocity of, say, 8,500 feet per second. The hodograph is as shown in figure 17 and indicates a hyperbolic trajectory. The pilot's task, in order to establish the specified orbit, is to reach the coordinates $\dot{R} = 0$, $R\dot{\theta} = 5{,}385$ at $h = 264{,}000$. He might logically attempt to move from the high-energy trajectory to the lower energy trajectory by properly matching velocities and altitudes. That is, he might move from point (A) to point (B) while the altitude was decreasing from 900,000 feet to 800,000 feet, then to point (C), and so on to the final coordinate. Various other schemes could be used. However, of the schemes considered, two appeared to be convenient and also efficient from the viewpoint of fuel consumption. These involved permitting the vehicle to trace the hodograph to some point where maximum available thrust could be applied continuously to put the vehicle into orbit. These two methods differ only in detail. In one, thrust is applied against the total velocity vector, and in the other, thrust is applied normal to the radius vector. In the first case, $\tan \alpha = \dot{R}/R\dot{\theta}$ and in the second case, $\tan \alpha = 0$. There was little difference between the two methods since $\dot{R}/R\dot{\theta}$ was quite small over the thrusting period. The thrust mode with $\alpha = 0$ was selected for use in this investigation.

The hodograph of the nominal ballistic trajectory selected for this investigation is shown in figure 8 and has a pericynthion velocity of 8,466 feet per second. Results from a digital computation showed that application of constant thrust (maximum value, corresponding to an initial T/m of 0.26 earth g unit) at an altitude of 383,700 would pass the hodograph trace through the coordinates $R\dot{\theta} = 5{,}385$ and $\dot{R} = 0$ at an altitude of 264,000 feet; thus, a 50-mile-altitude circular orbit would be established.

The hodograph presentation would also have been very useful had an alternate thrust mode (thrust against the velocity vector) been adopted. Since in this mode $\alpha = \tan^{-1}\left(\dot{R}/R\dot{\theta}\right)$, the value of α can be read directly from radial lines through the origin of the hodograph. The radial lines could be drawn on the hodograph as done in figure 18 or put on an overlay.

There is yet another hodograph display which might be of interest, and this would answer the following question: If thrust is terminated and the vehicle permitted to follow a ballistic course, will the vehicle pass the moon or will it impact? The hodograph in this instance consists of constant altitude lines which represent velocity combinations required to skim the lunar surface (neglecting surface perturbances). (See fig. 19.) For a given altitude, velocity combinations above the constant-altitude line indicated no impact, whereas velocity combinations below the line indicate an impact.

REFERENCES

1. Grube, Robert H.: Terminal Guidance for Lunar and Planetary Probes. Proc. Nat. Specialists Meeting on Guidance of Aerospace Vehicles (Boston, Mass.), Inst. Aero. Sci., May 1960, pp. 178-183.

2. Hendrix, Charles E.: Proposal for a Simple System for Achieving Soft Landing of a Rocket Vehicle. NAVWEPS Rep. 7084 (AD No. 239357), U.S. Naval Ord. Test Station (China Lake, Calif.), June 8, 1960.

3. Weber, Richard J., and Pauson, Werner M.: Some Thrust and Trajectory Considerations for Lunar Landings. NASA TN D-134, 1959.

4. Carton, D. S.: Minimum Propulsion for Soft Moon Landing of Instruments. Note No. 94, The College of Aeronautics, Cranfield (British), July 1959.

5. Moeckel, W. E.: Trajectories With Constant Tangential Thrust in Central Gravitational Fields. NASA TR R-53, 1960.

6. Michael, William H., Jr., and Tolson, Robert H.: Three-Dimensional Lunar Mission Studies. NASA MEMO 6-29-59L, 1959.

7. Creer, Brent Y., Smedal, Harald A., and Wingrove, Rodney C.: Centrifuge Study of Pilot Tolerance to Acceleration and the Effects of Acceleration on Pilot Performance. NASA TN D-337, 1960.

8. Andrews, William H., and Holleman, Euclid C.: Experience With a Three-Axis Side-Located Controller During a Static and Centrifuge Simulation of the Piloted Launch of a Manned Multistage Vehicle. NASA TN D-546, 1960.

L
1
5
2
3

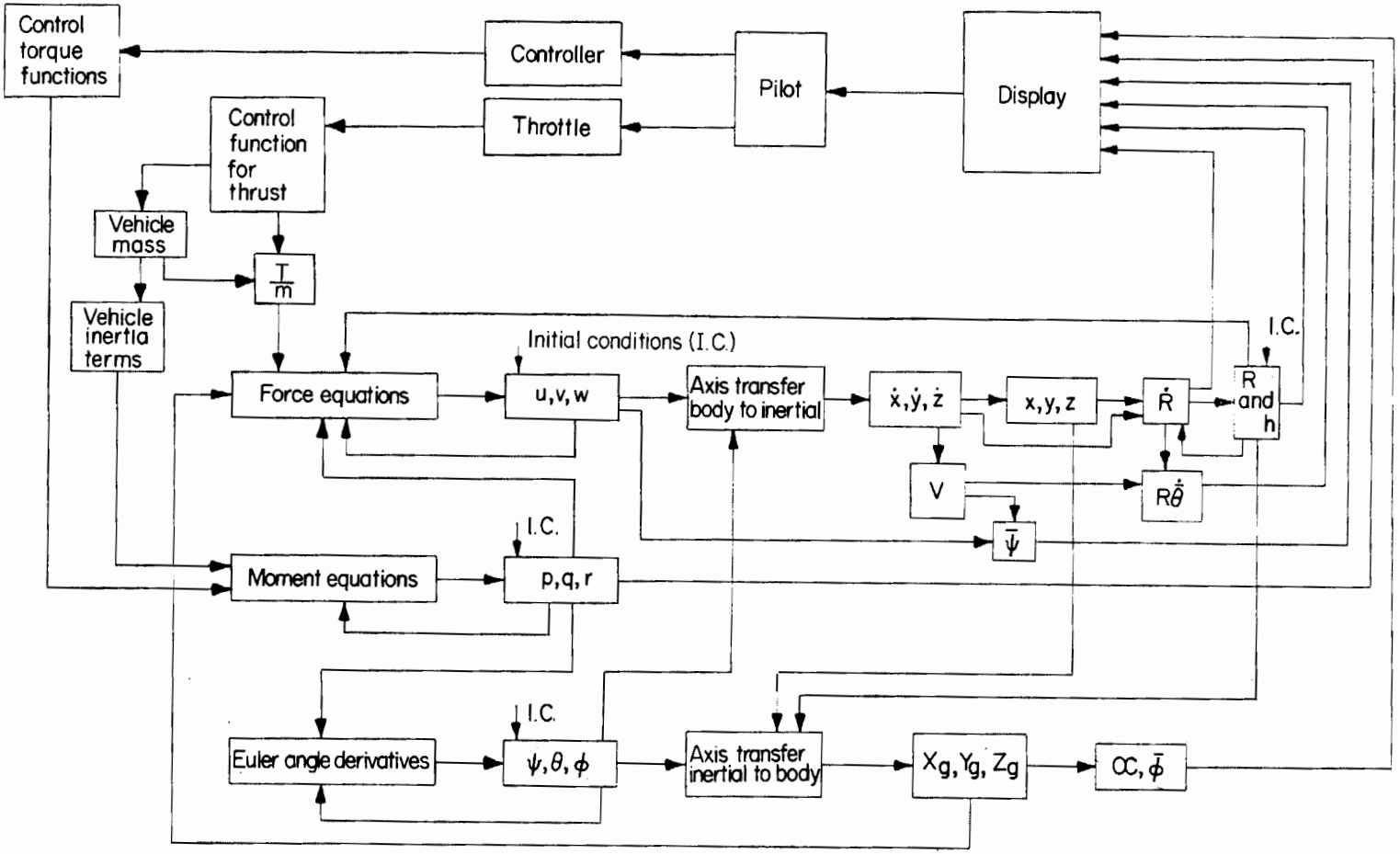

Figure 1.- Block diagram of equations showing information flow of computer program.

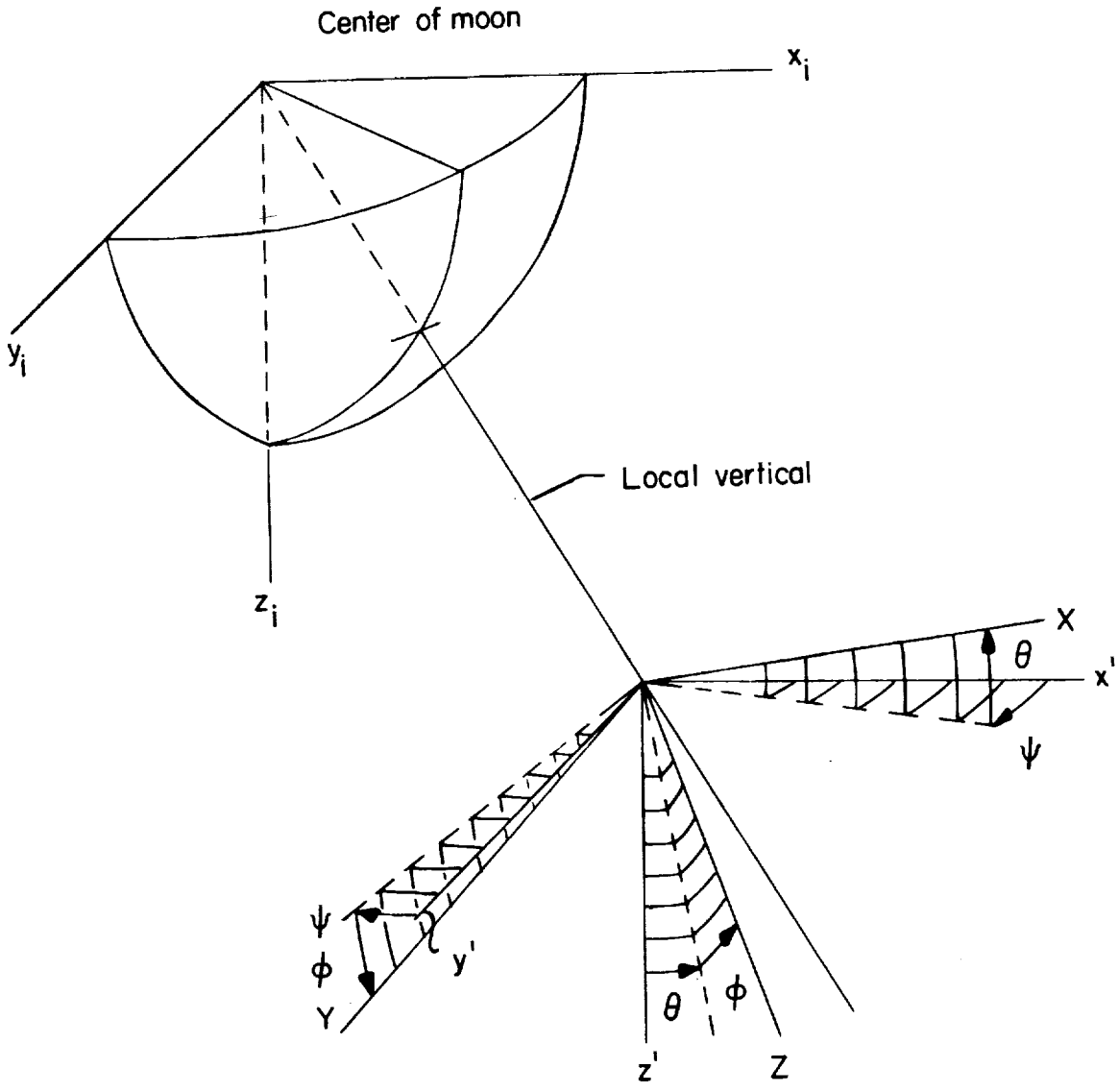

(a) Inertial and vehicle axes systems showing positive rotations and linear displacements of vehicle.

Figure 2.- Axes systems and angles used.

L-1523

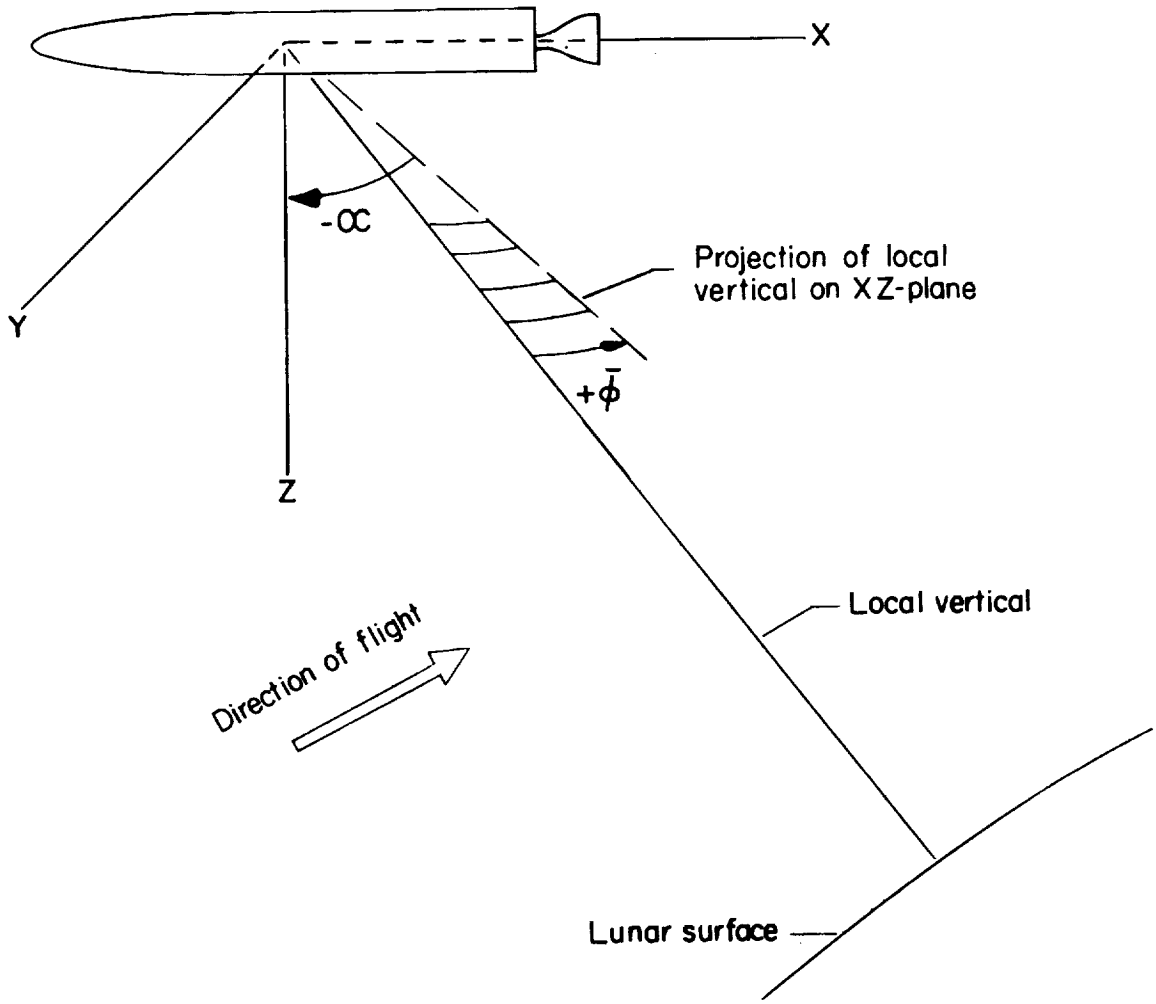

(b) Vehicle attitude angles α and $\bar{\phi}$ and vehicle orientation relative to body-axis system.

Figure 2.- Concluded.

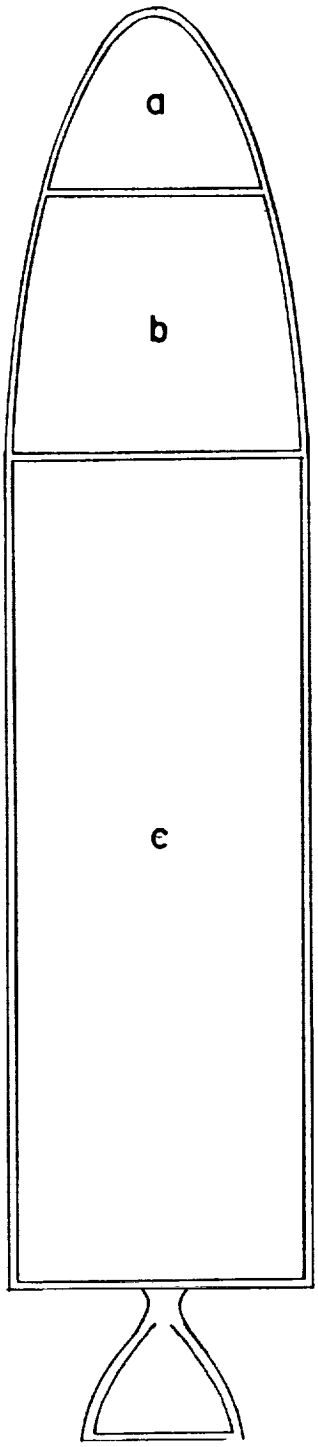

a Guidance

b Living quarters and controls

c Propellant

Vehicle characteristics

	Initial value	Approximate value at orbit attainment
$\frac{m}{m_0}$	1.0000	0.7000
$\frac{T}{m}$	8.2418	11.3297
$\frac{I_X}{I_Y}$	.1908	.2334
$\frac{I_Y-I_X}{I_Y}$	.8092	.7666
$\frac{\dot{I}_X}{I_X}$	0	-.0006
$\frac{\dot{I}_Y}{I_Y}$	-.0007	-.0011

Figure 3.- Assumed vehicle.

L-1523

Figure 4.- Cockpit used for simulation study. L-60-7360

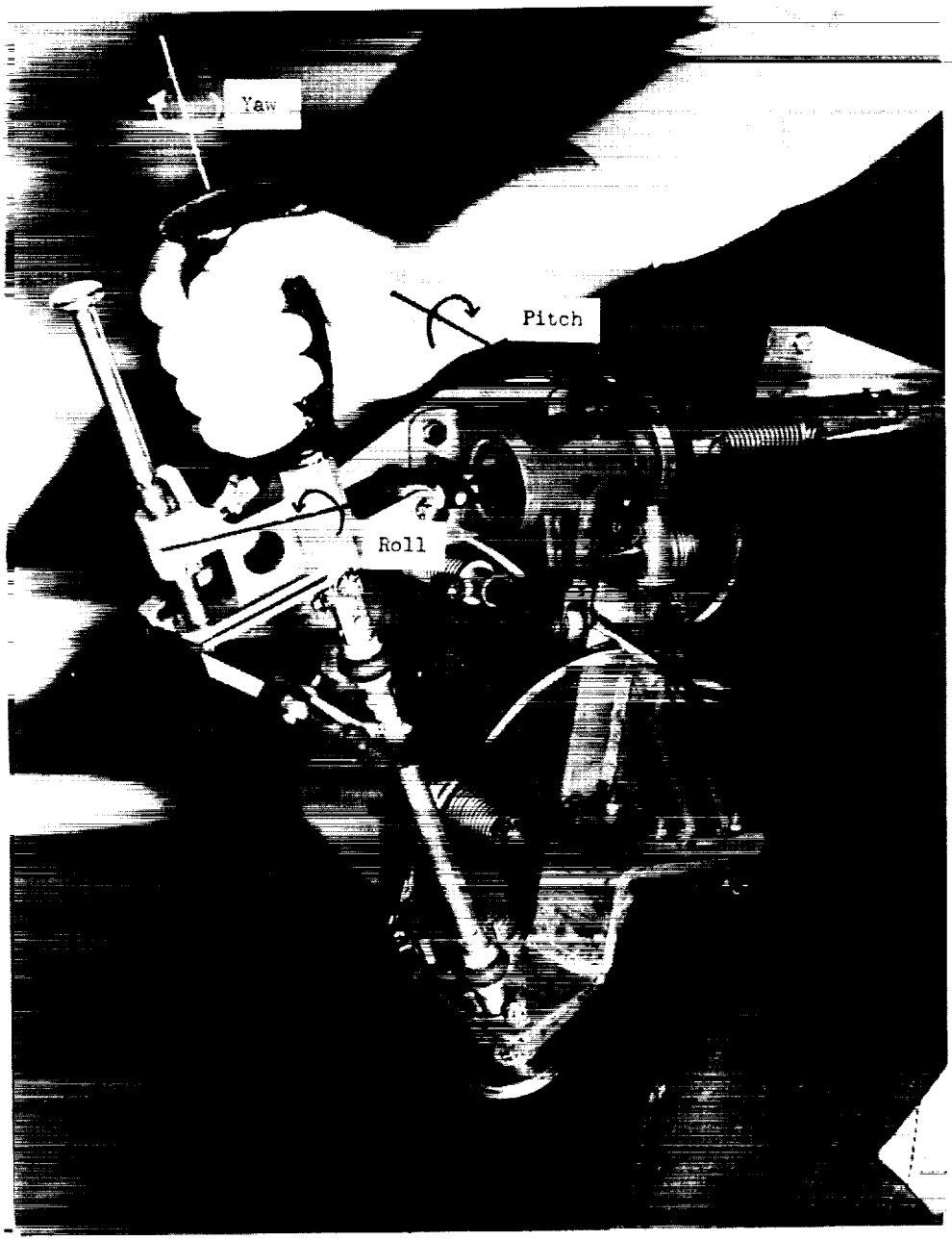

L-59-7121.1

(a) A closeup photograph of the three-axis hand controller showing location of axes of rotation of mechanism.

Figure 5.- The three-axis hand controller and the associated control-torque functions employed.

L-1523

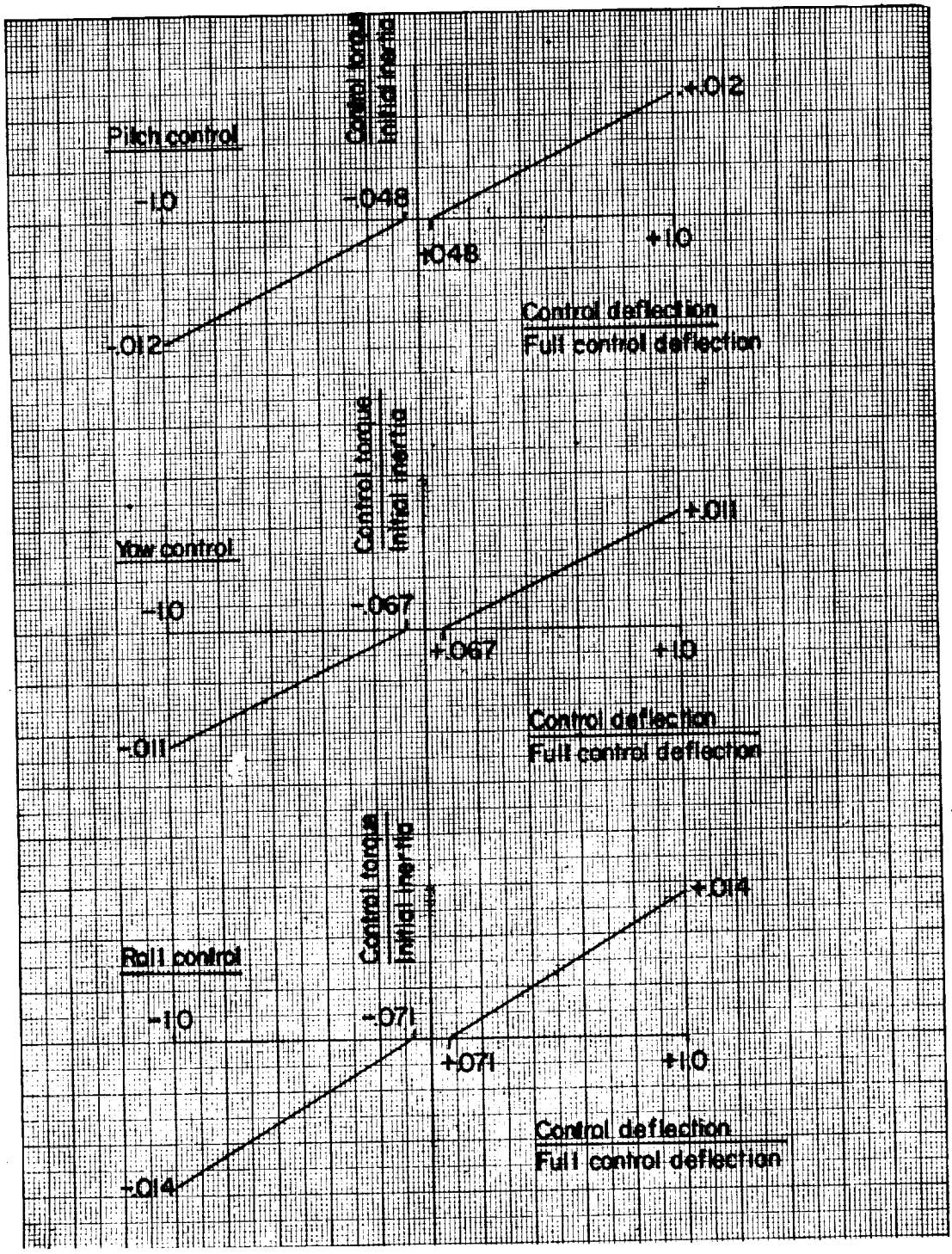

(b) Variations of control torque with controller deflection.

Figure 5.- Concluded.

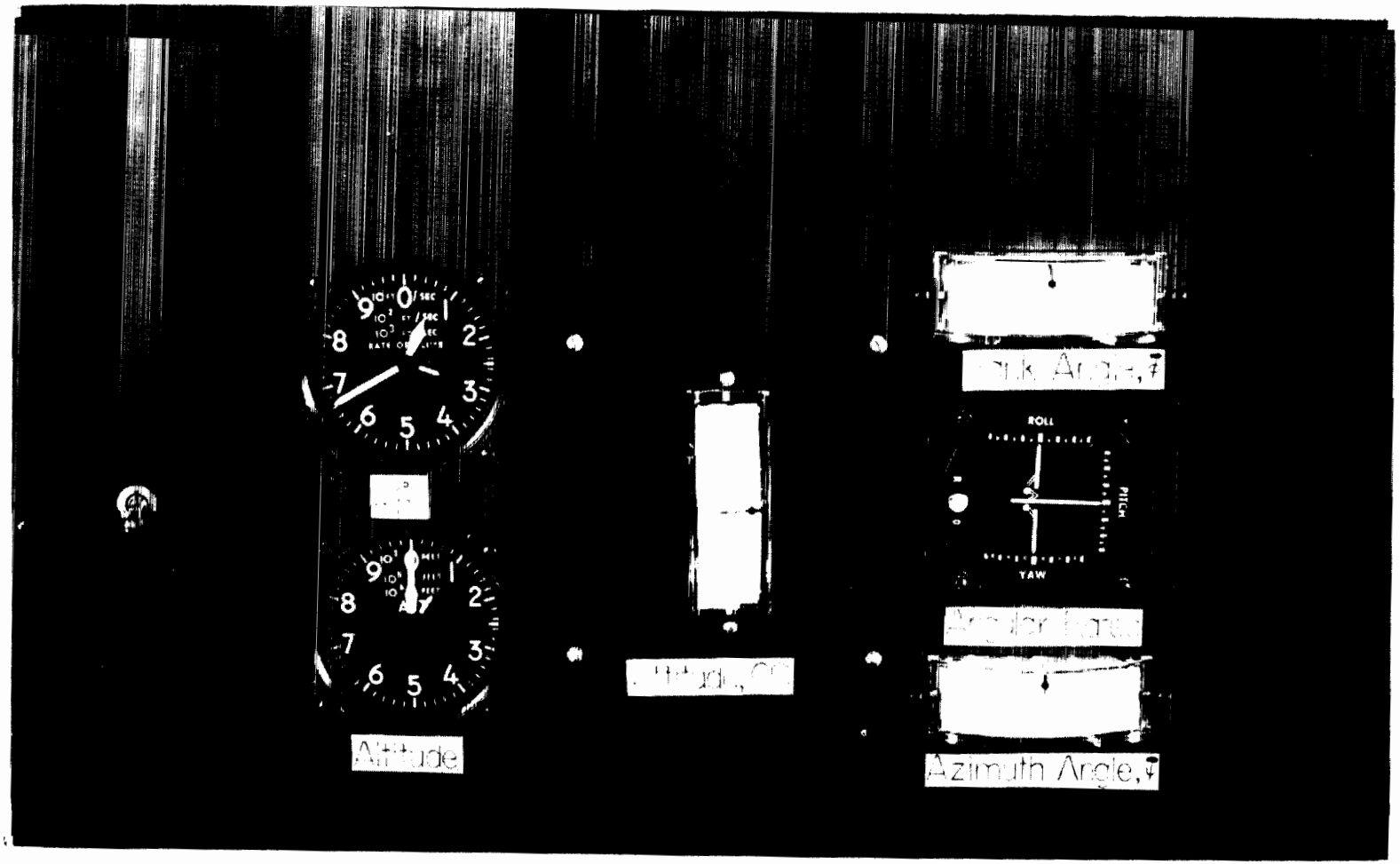

Figure 6.- A closeup photograph of instrument panel. L-60-7361

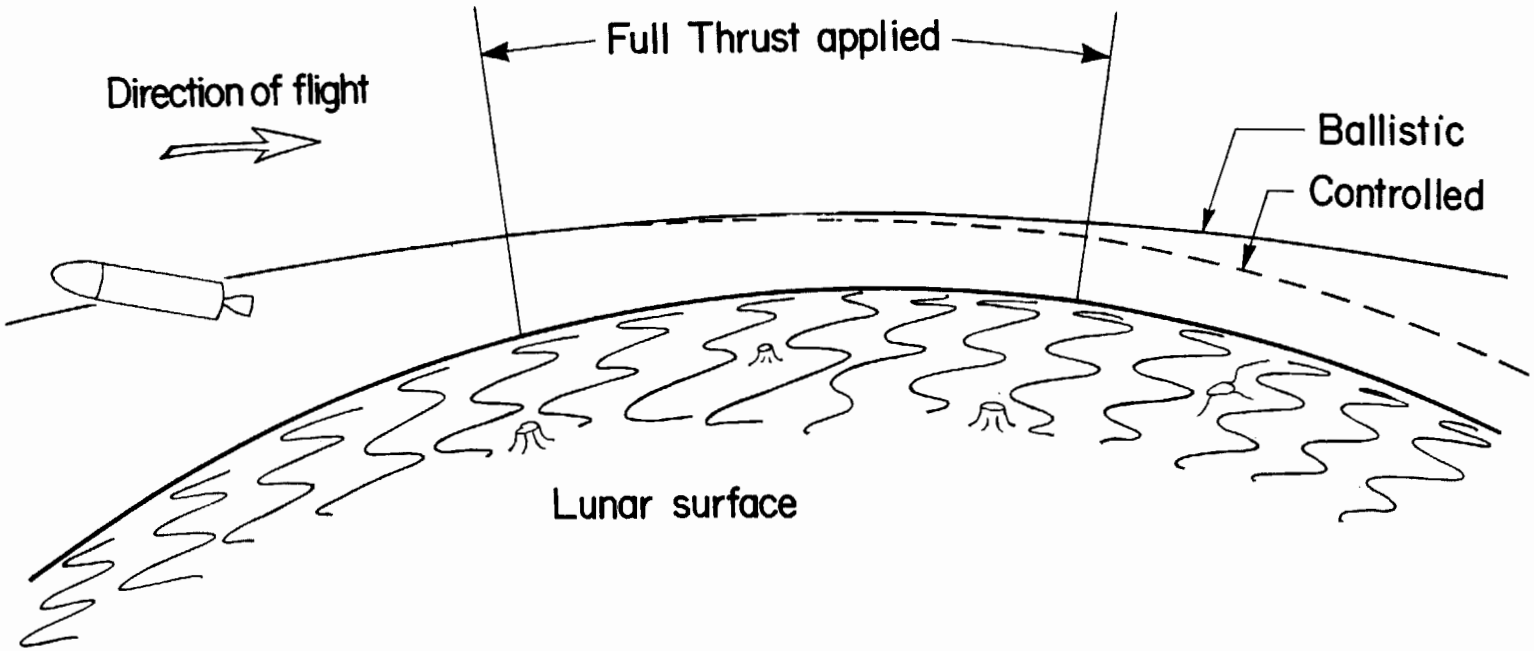

Figure 7.- Ballistic and controlled flight paths.

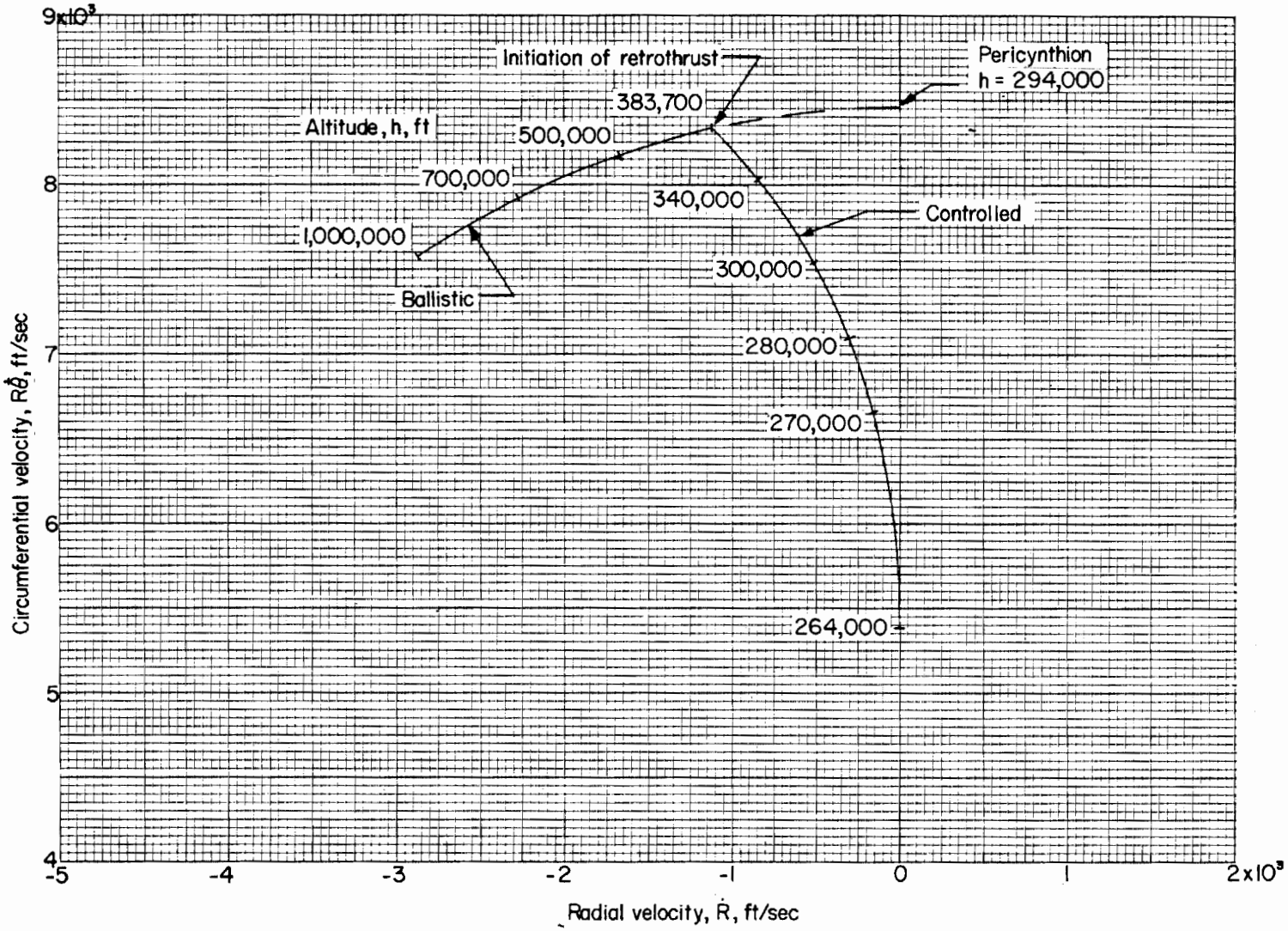

Figure 8.- Nominal trajectory in hodograph plane.

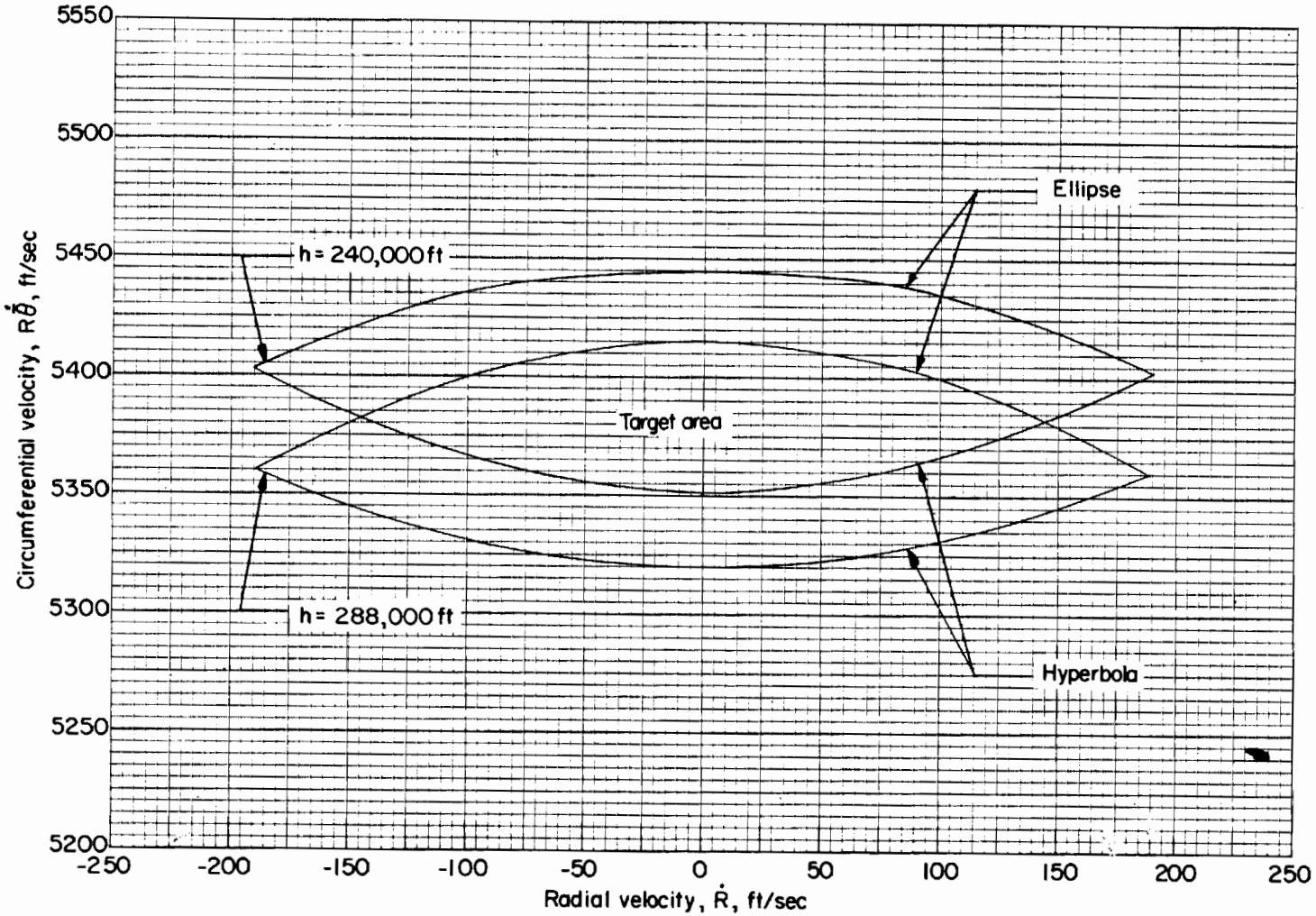

Figure 9.- Computed target area in the hodograph that specifies vehicle altitude and velocity components required at thrust termination for lunar orbits lying within 10- to 90-mile altitude range.

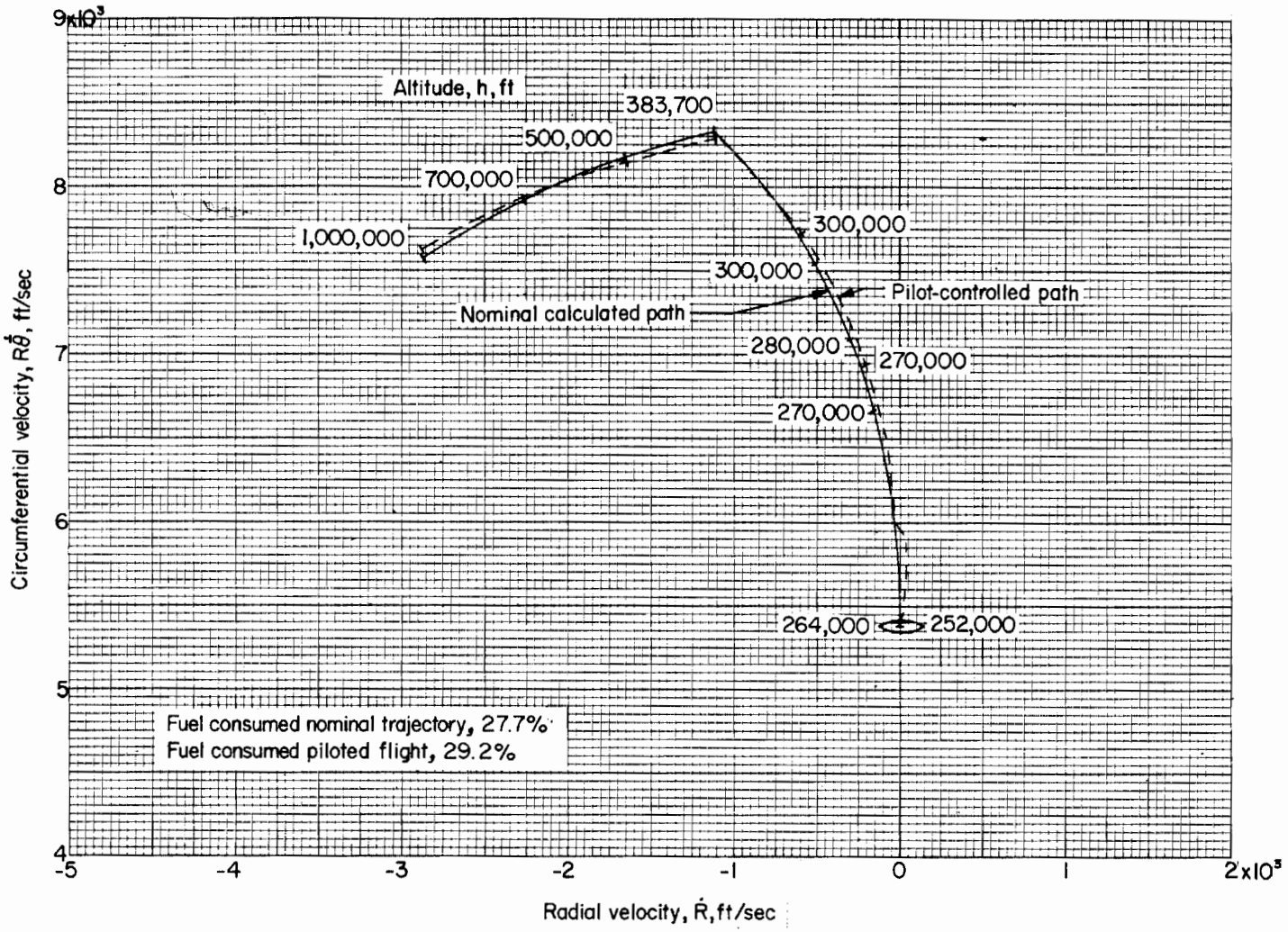

Figure 10.- Typical piloted flight of the nominal trajectory (fuel consumption given in percent of initial vehicle mass).

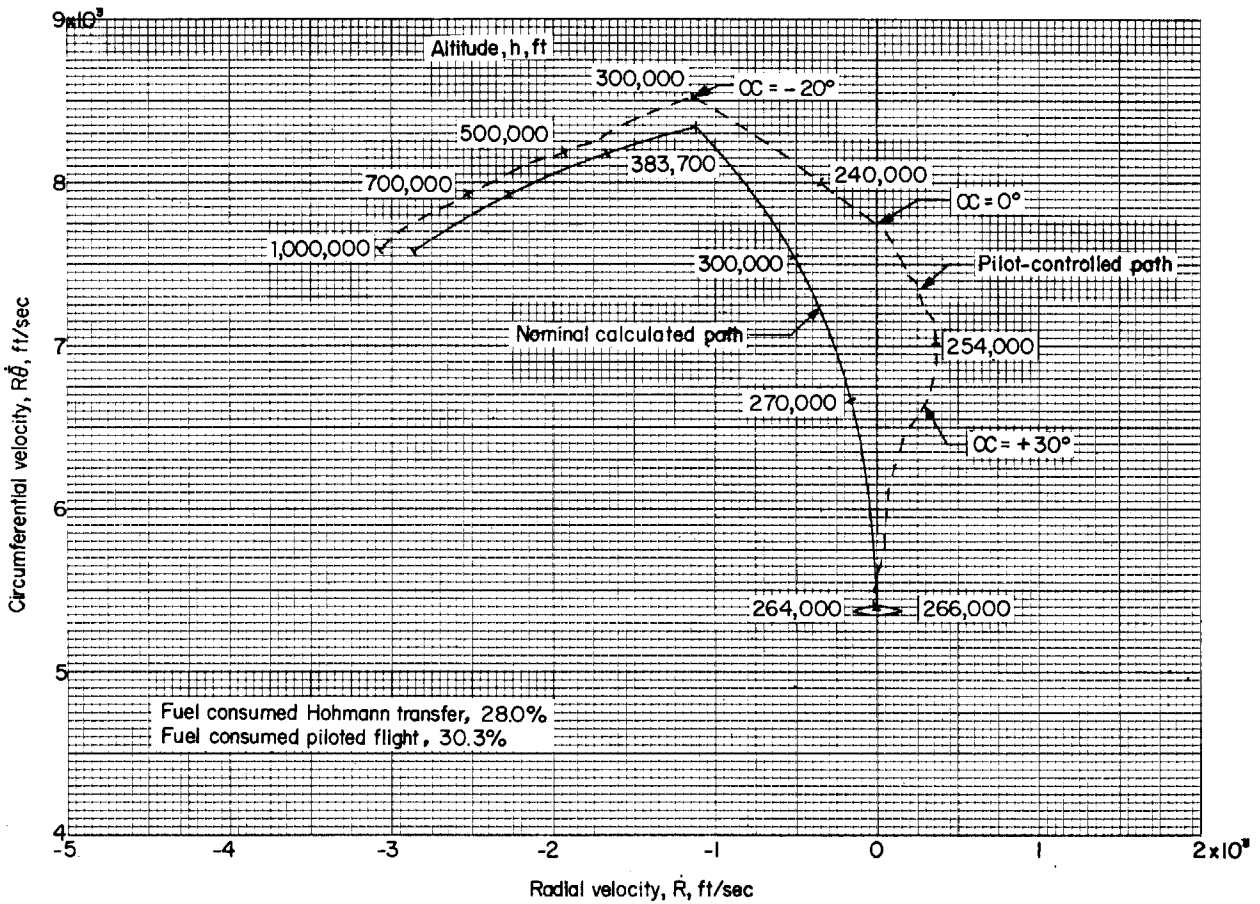

(a) Hodograph.

Figure 11.- Piloted flight of an off-nominal trajectory during which full thrust was applied continuously from thrust initiation until vehicle achieved desired orbital conditions. Thrust initiation altitude, 300,000 feet. (Fuel consumption given in percent of initial vehicle mass.)

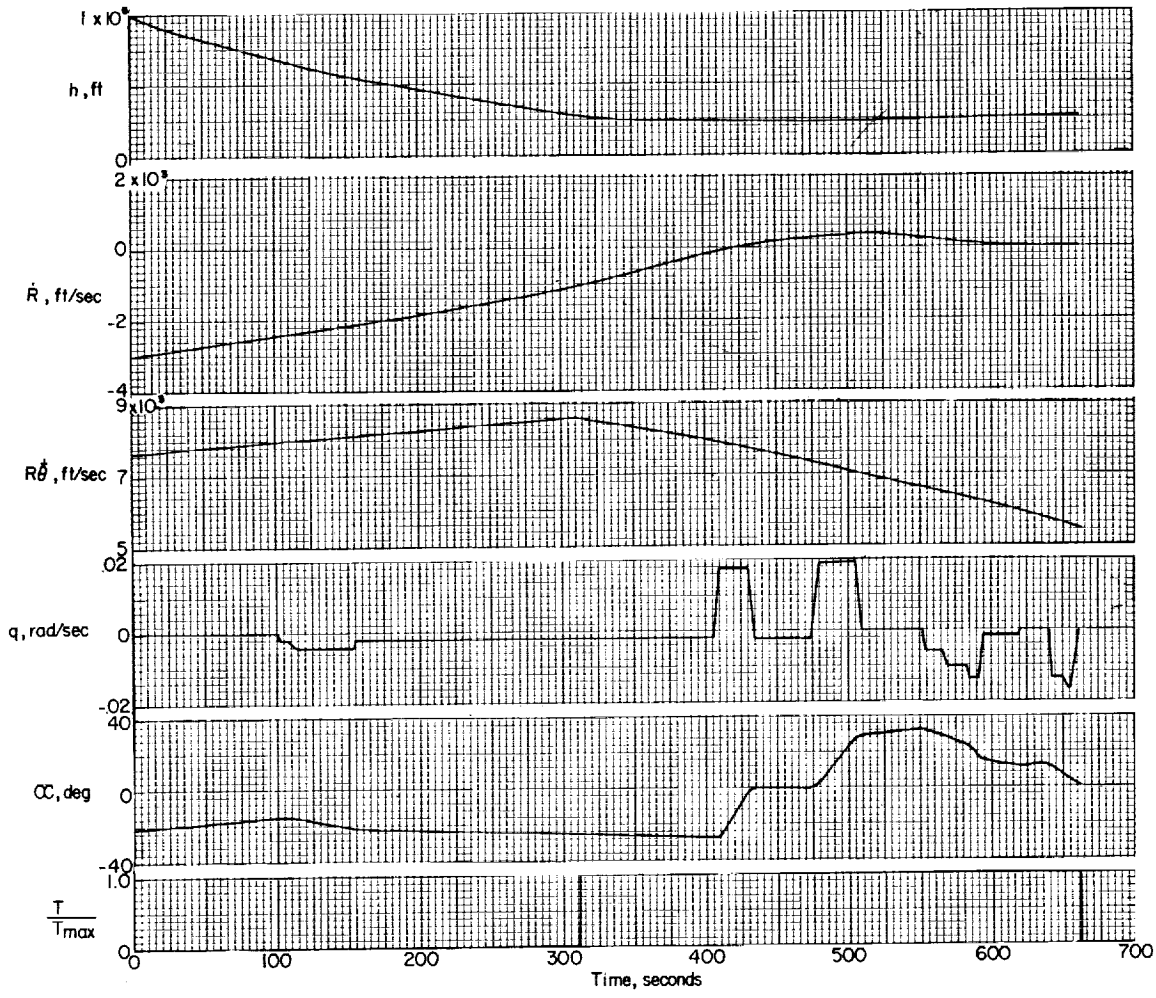

(b) Time histories.

Figure 11.- Concluded.

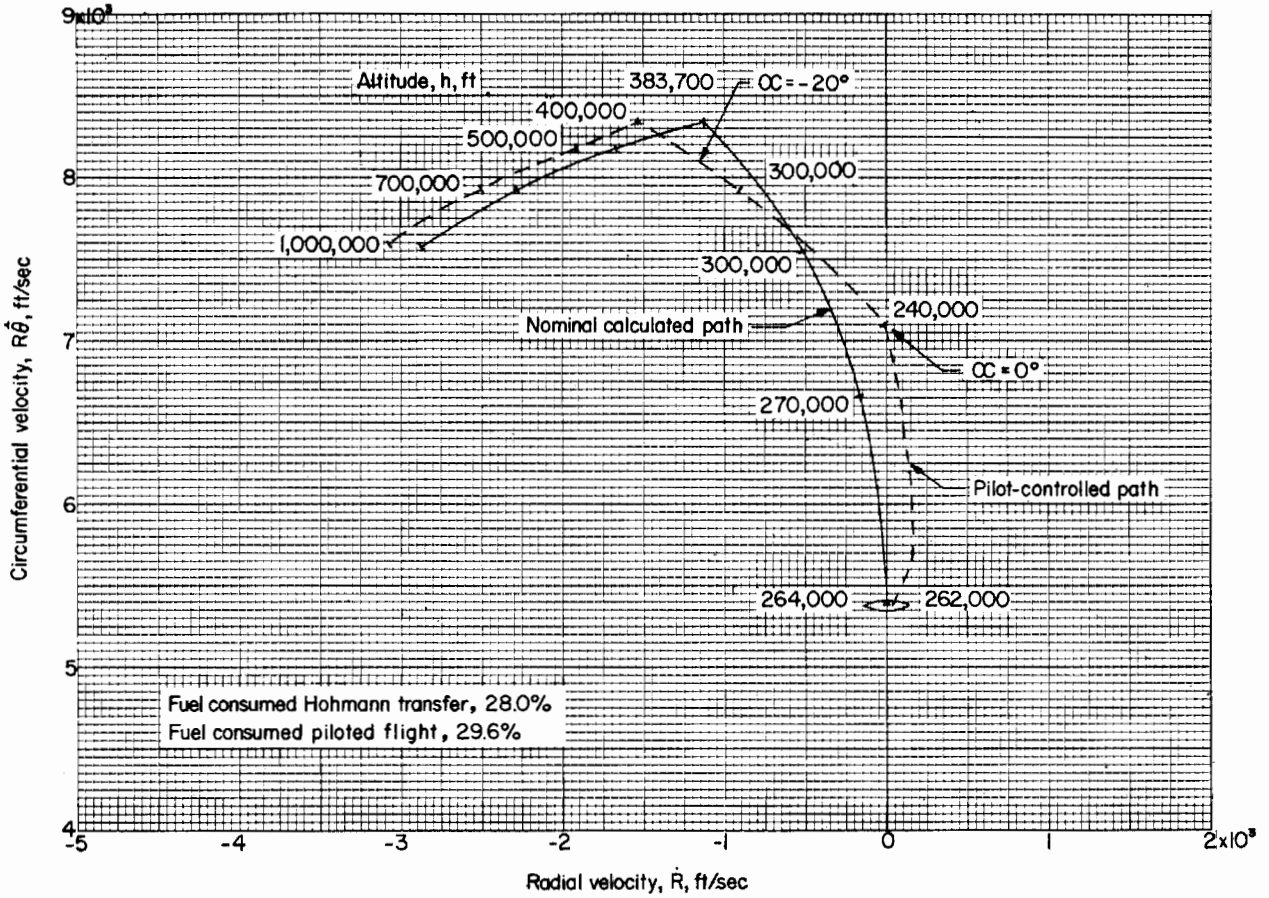

(a) Hodograph.

Figure 12.- Piloted flight of an off-nominal trajectory during which full thrust was applied continuously from thrust initiation until the vehicle achieved the desired orbital conditions. Thrust initiation altitude, 400,000 feet. (Fuel consumption given in percent of initial vehicle mass.)

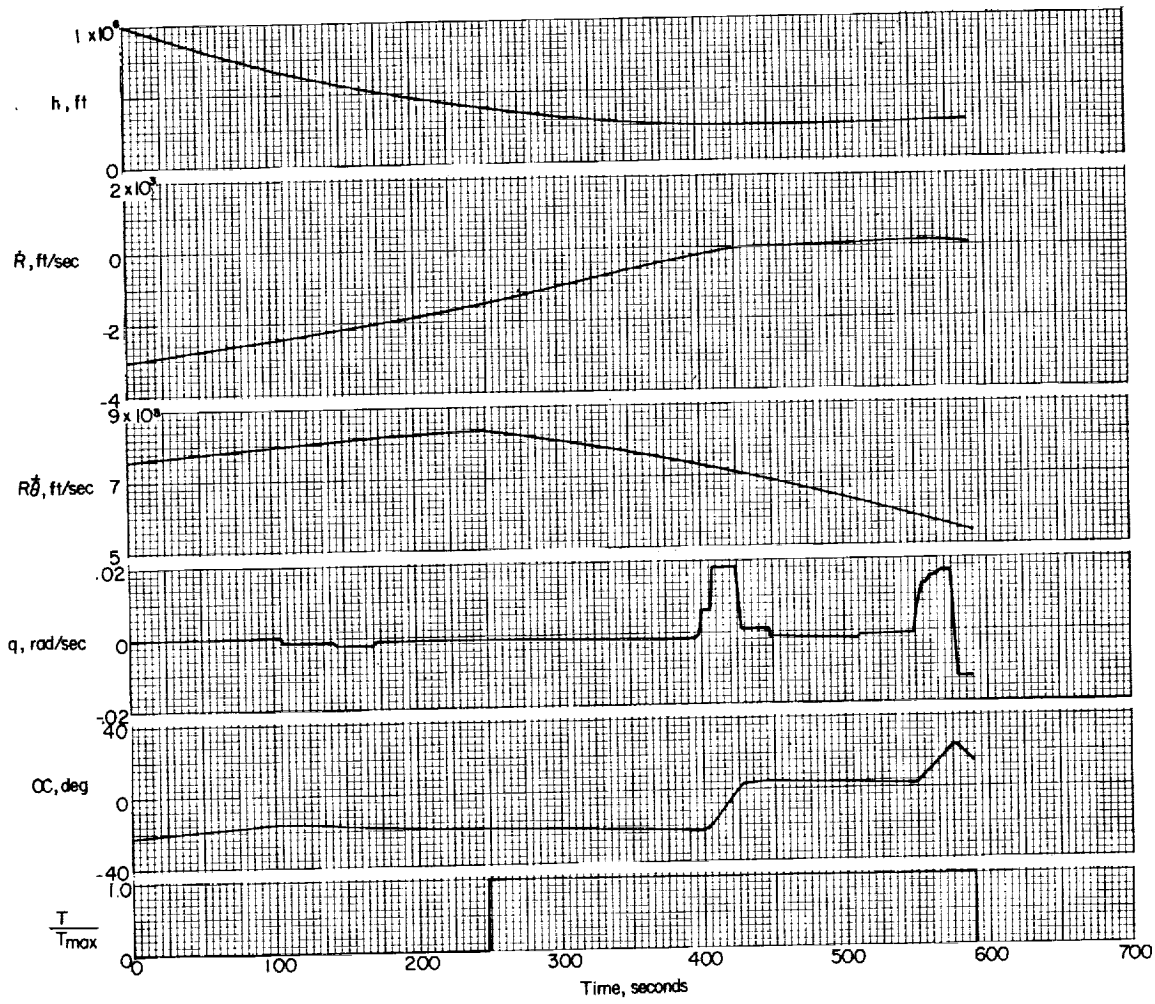

(b) Time histories.

Figure 12.- Concluded.

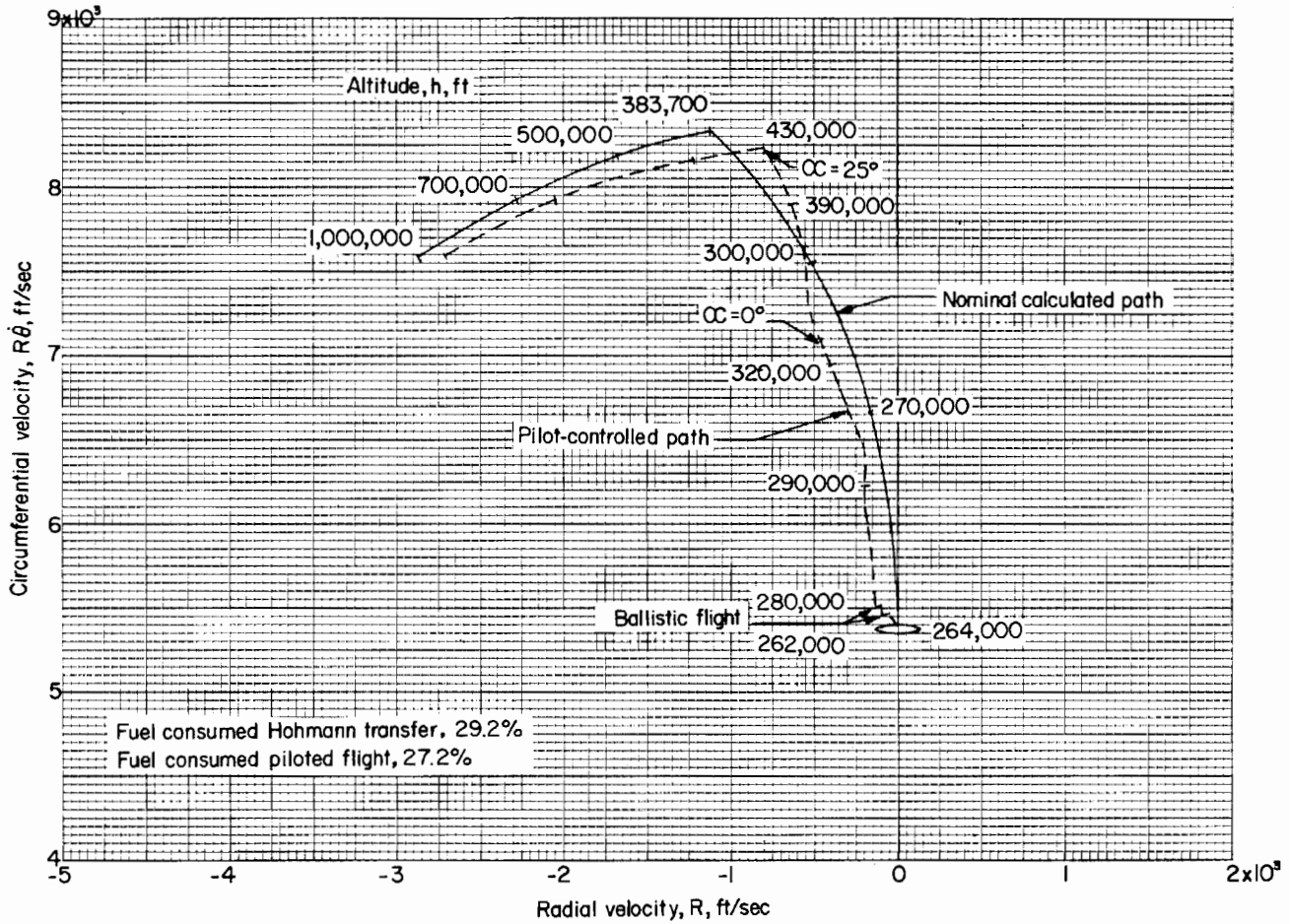

(a) Hodograph.

Figure 13.- Piloted flight of an off-nominal trajectory during which thrust was terminated for brief periods in order to achieve the desired orbital conditions. (Fuel consumption given in percent of initial vehicle mass.)

(b) Time histories.

Figure 13.- Concluded.

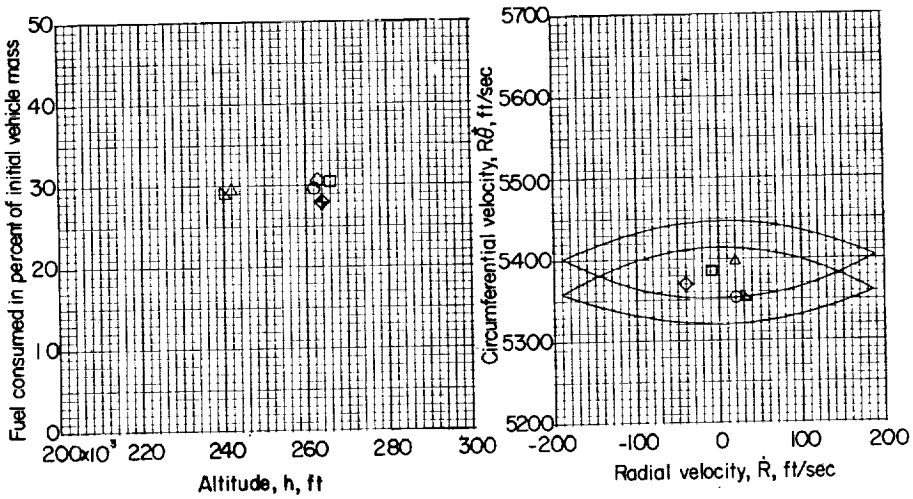

(a) Flights initiated at an altitude of 1×10^6 feet, $R\dot{\theta}$ nominal (7,575 ft/sec), and rate of descent 200 ft/sec greater than nominal value ($\dot{R}$ = -3,067 ft/sec).

◆ Calculated Hohmann transfer

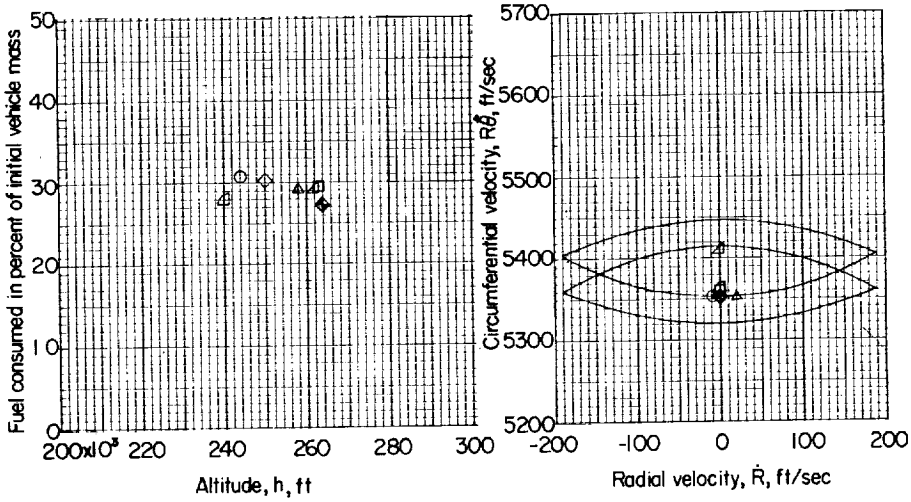

(b) Flights initiated at an altitude of 1×10^6 feet, $R\dot{\theta}$ nominal (7,575 ft/sec), and rate of descent 200 ft/sec less than nominal value ($\dot{R}$ = -2,667 ft/sec).

Figure 14.- Fuel consumption, altitude, and vehicle velocity components achieved at the end of piloted flight for a number of off-nominal trajectories flown from different initial conditions. Different symbols indicate different flights.

L-1523

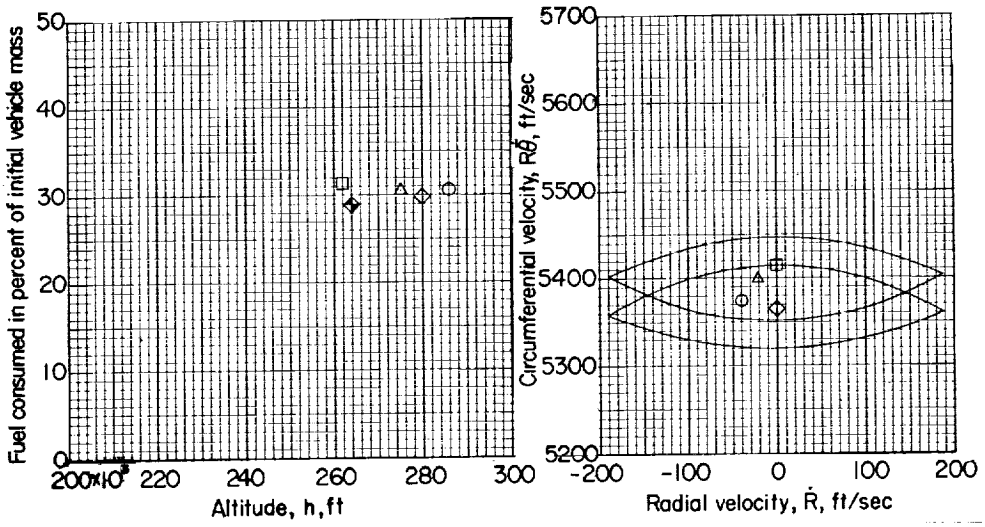

(c) Flight initiated at an altitude of 1×10^6 feet, $\dot{R}$ nominal ($\dot{R}$ = -2,867 ft/sec), and $R\dot{\theta}$ = 200 ft/sec greater than nominal value (7,775 ft/sec).

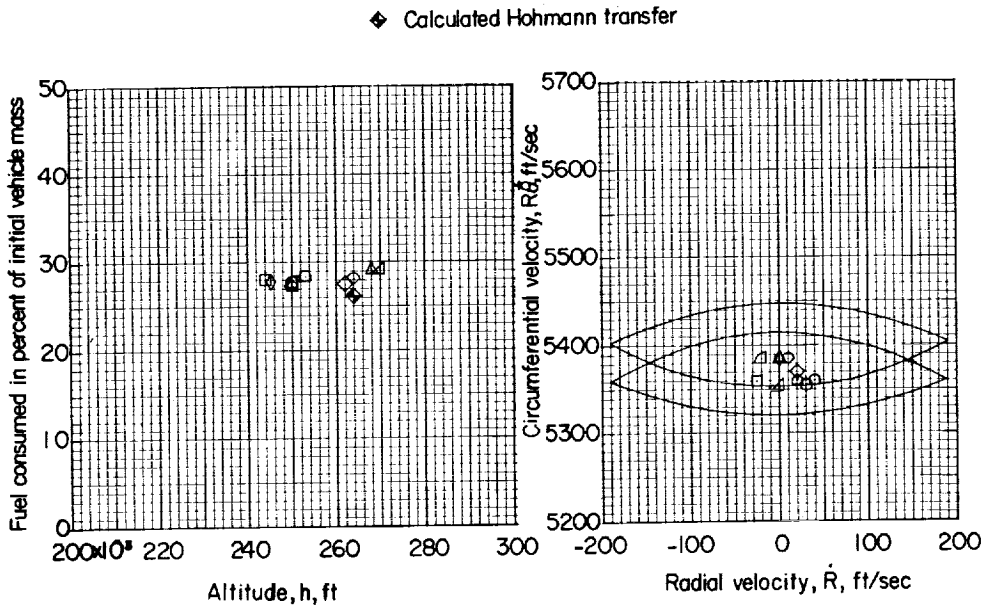

(d) Flight initiated at an altitude of 1×10^6 feet, $\dot{R}$ nominal ($\dot{R}$ = -2,867 ft/sec), and $R\dot{\theta}$ = 200 ft/sec less than nominal value (7,375 ft/sec).

Figure 14.- Concluded.

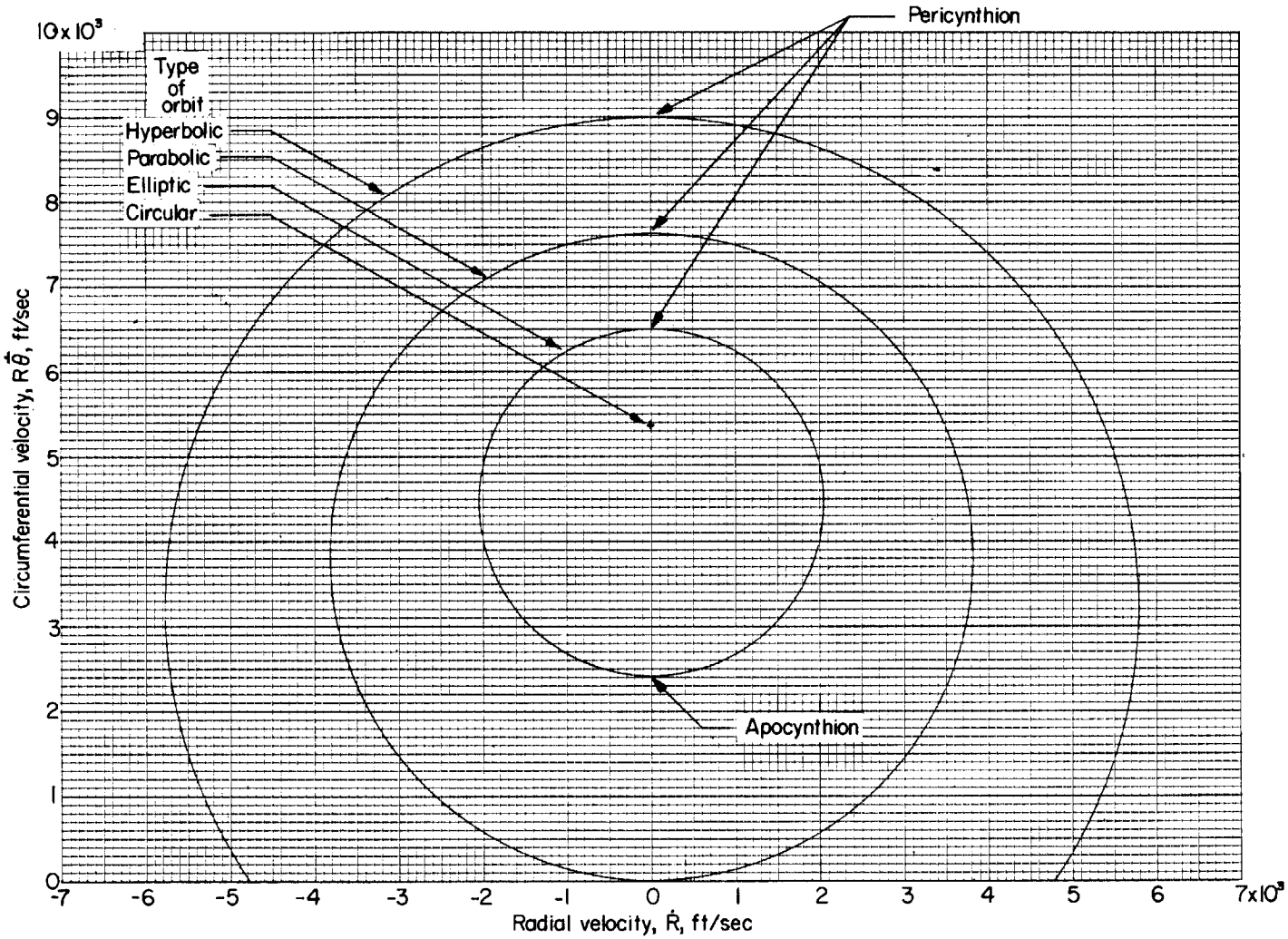

Figure 15.- Typical traces of various types of trajectories on hodograph plane (values shown are for pericynthion altitudes of 50 statute miles).

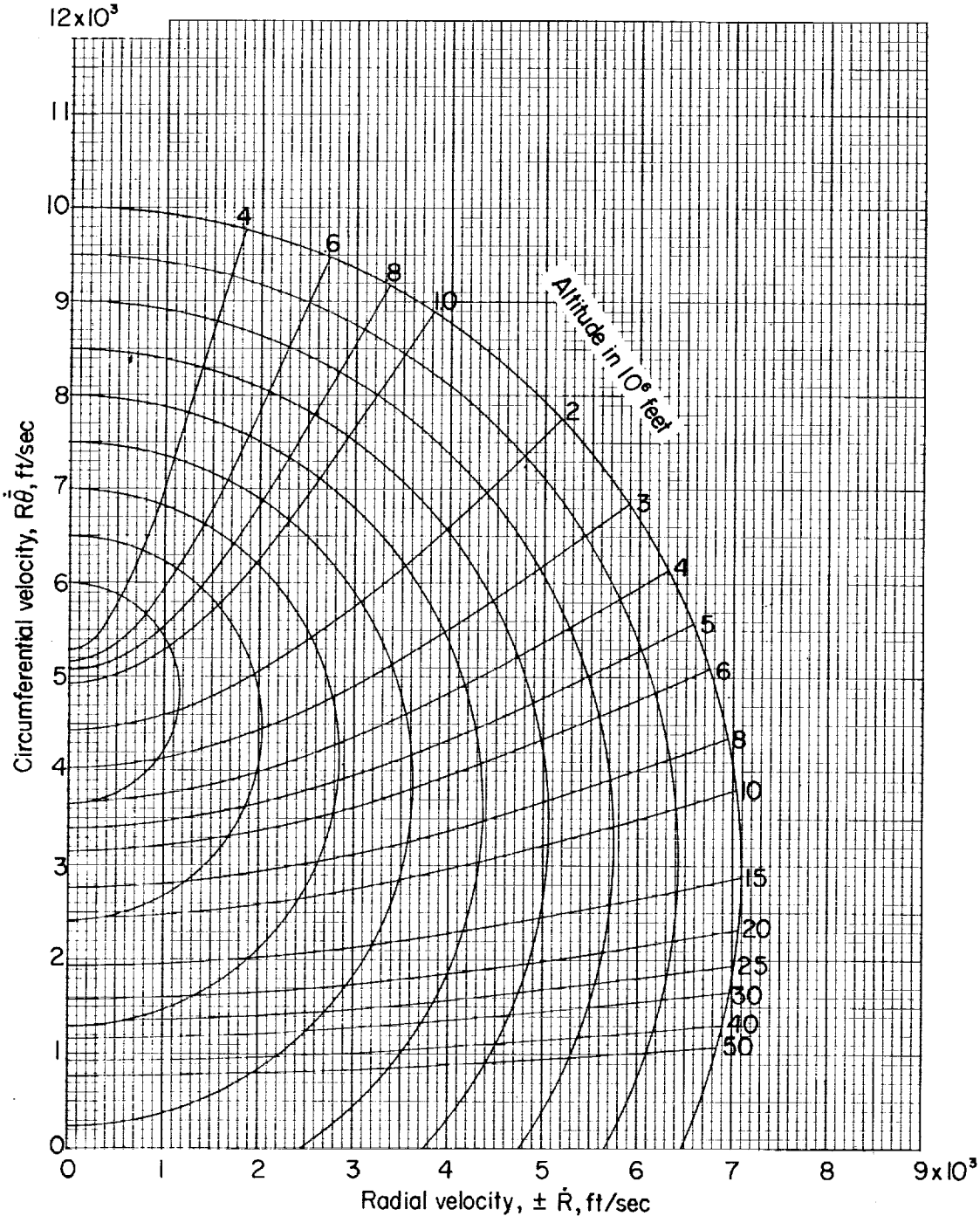

Figure 16.- Hodograph of trajectories having a pericynthion altitude of 50 miles.

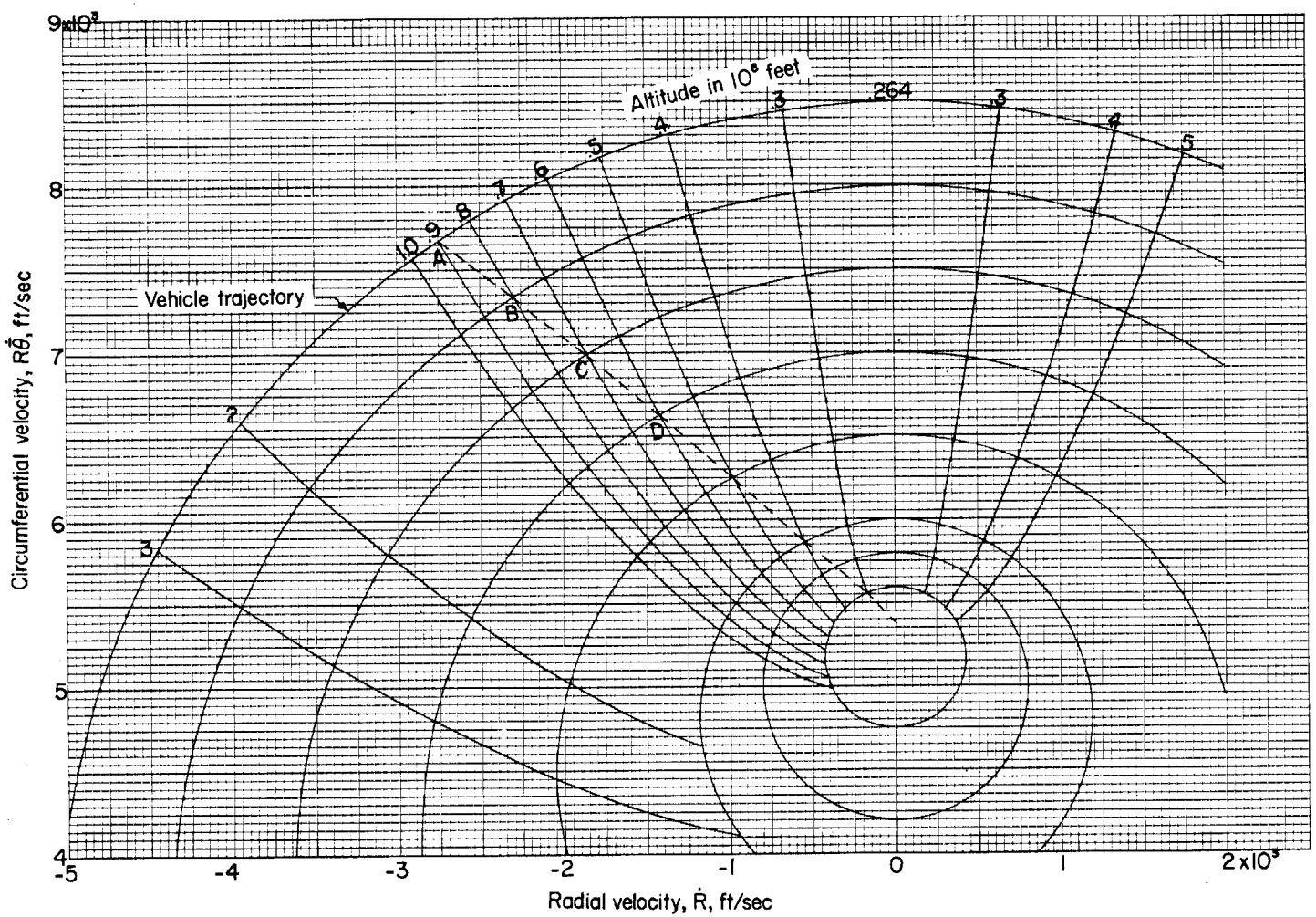

Figure 17.- Hodograph for pericynthion altitude of 50 miles illustrating a step-by-step procedure for establishing a circular orbit by thrusting so as to match velocity and altitude conditions at successive points A, B, C, D, and so on.

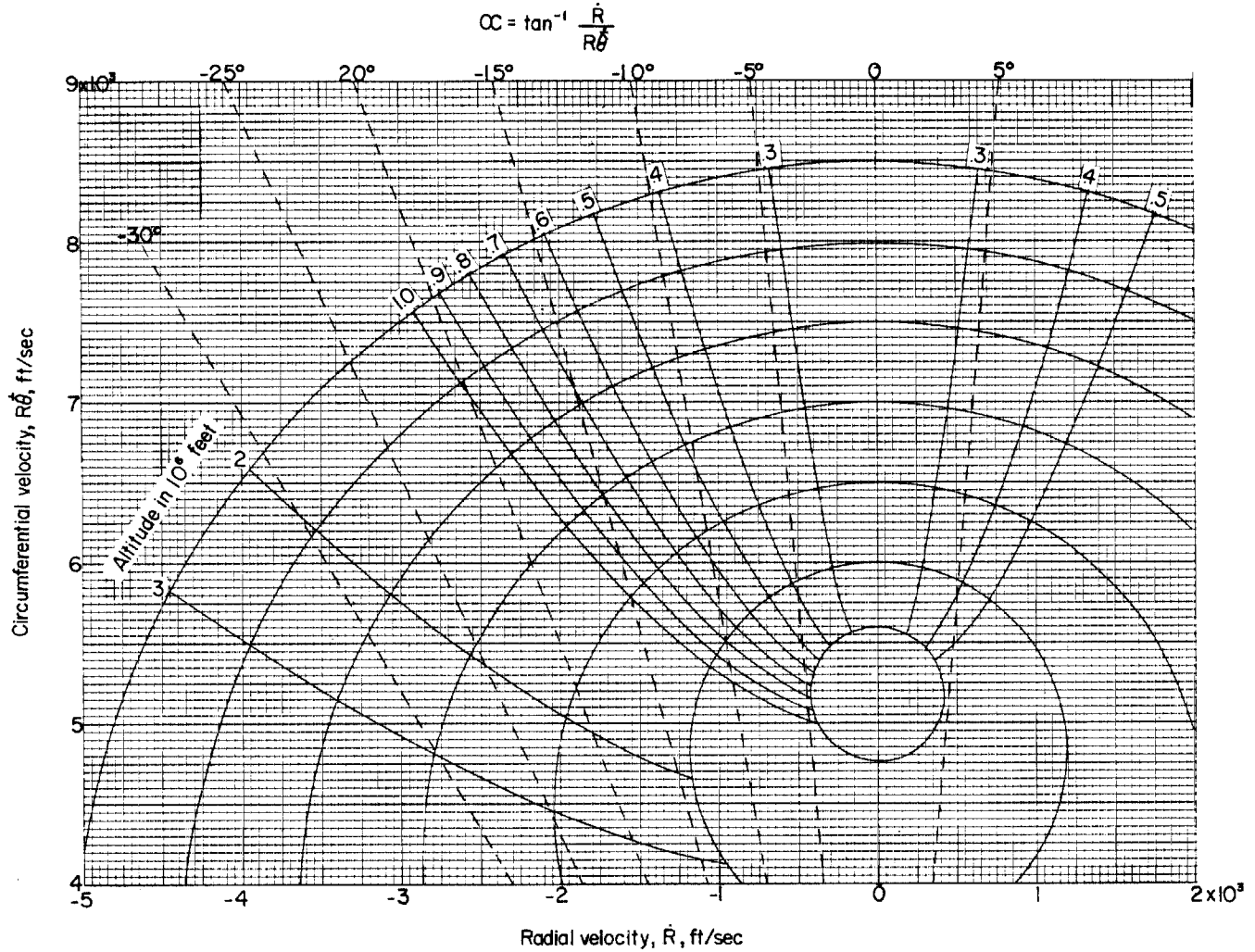

Figure 18.- Hodograph showing vehicle pitch angle α required for thrusting directly against velocity vector.

NASA - Langley Field, Va. L-1523

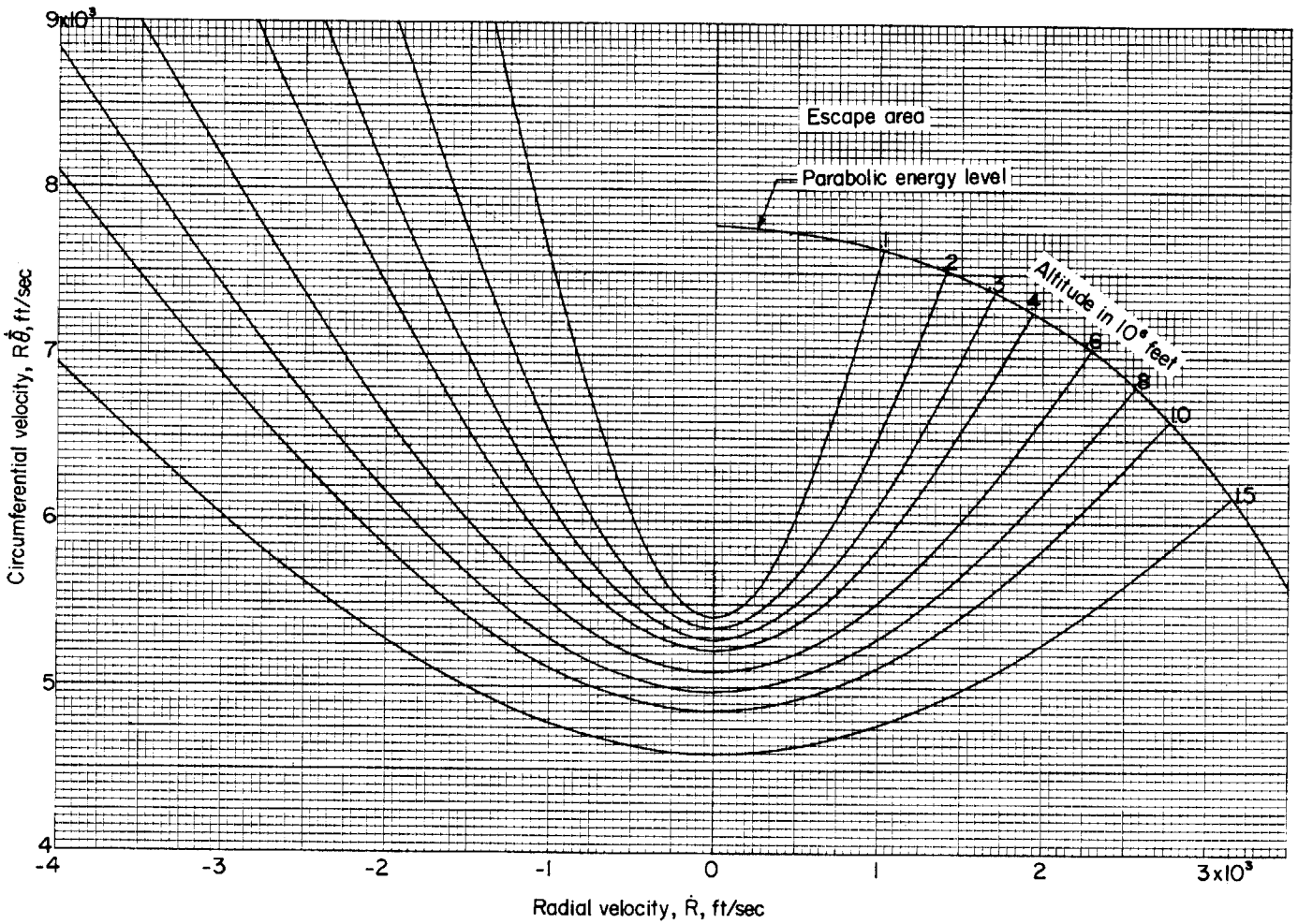

Figure 19.- Hodograph presentation showing miss boundaries for ballistic flight. For a given altitude, velocity combinations falling below the altitude line result in impact, those on the altitude line skim the lunar surface, and those above the altitude line miss the surface.